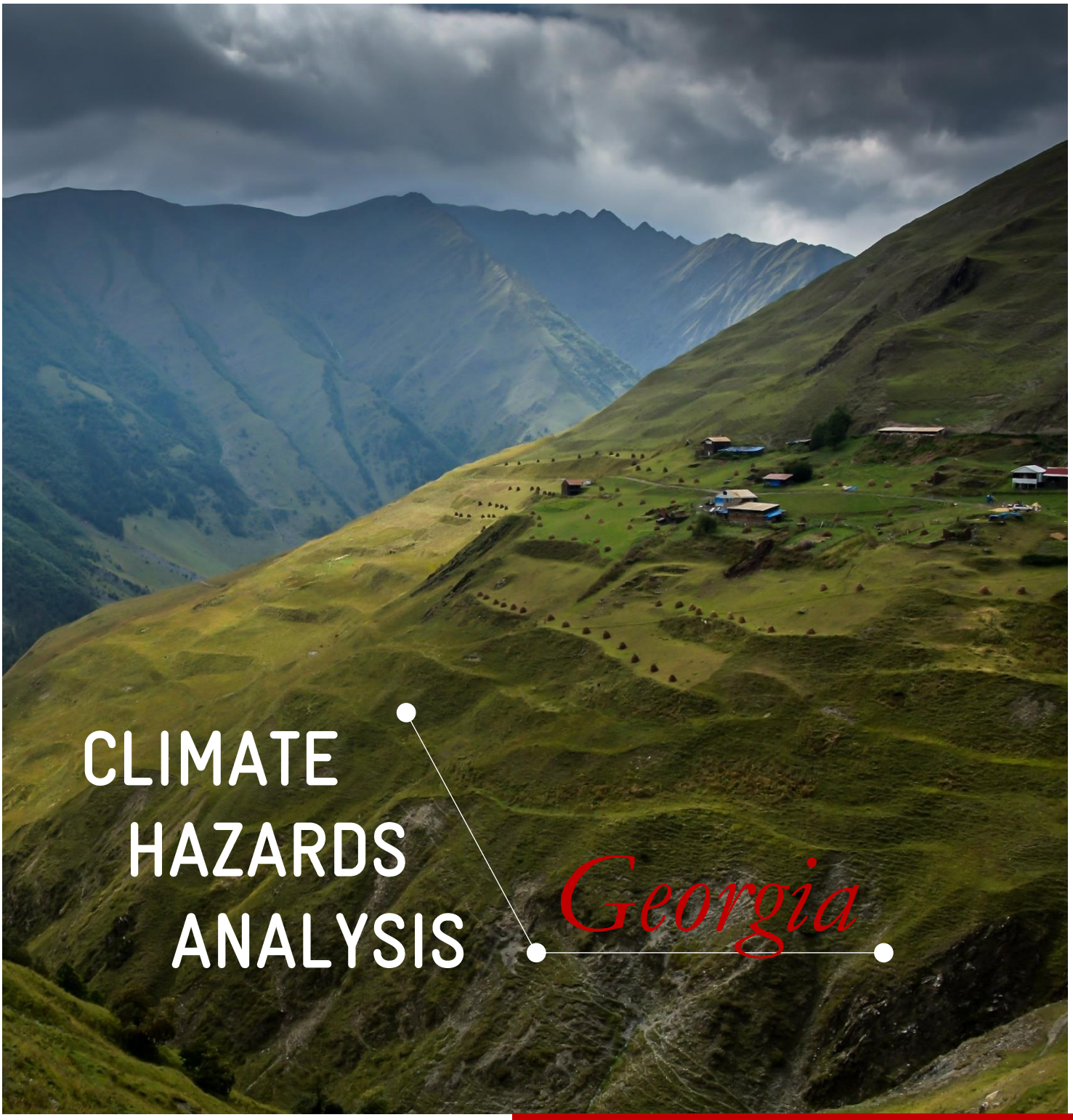

# CLIMATE HAZARDS ANALYSIS

*Georgia*

Global Programme on Policy Advice for Climate Resilient Economic Development


giz Deutsche Gesellschaft für Internationale Zusammenarbeit (GIZ) GmbH

On behalf of:

Federal Ministry for the Environment, Nature Conservation and Nuclear Safety

of the Federal Republic of Germany

UIB Universitat de les Illes Balears

# REPORT ON THE CLIMATE HAZARDS ANALYSIS FOR GEORGIA

As a federally owned enterprise, GIZ supports the German Government in achieving its objectives in the field of international cooperation for sustainable development.

Published by:
Deutsche Gesellschaft für
Internationale Zusammenarbeit (GIZ) GmbH

Registered offices:
Bonn and Eschborn, Germany

Address:
Deutsche Gesellschaft für
Internationale Zusammenarbeit (GIZ) GmbH
Köthener Str. 2
10963, Berlin, Germany
T +49 61 96 79-0
F +49 61 96 79-11 15
E info@giz.de
I www.giz.de/en

Programme/project description:
IKI Global Programme on
Policy Advice for Climate Resilient Economic Development (CRED)

Project Director:
Stefanie Springorum
stefanie.springorum@giz.de

Authors:
Javier Soto Navarro, Mediterranean Institute for Advances Studies, Spain
Gabriel Jorda, Spanish Institute of Oceanography (IEO), Spain

Editor:
Patrick Zuell, Berlin

Design/layout, etc.:
Alvira Yertayeva, Nur-Sultan

Photo sources:
pixabay.com

The report "Climate Hazards Analysis for Georgia" was developed by the experts of Mediterranean Institute for Advances Studies (IMEDEA, UIB-CSIC) and Spanish Institute of Oceanography (IEO) in the framework of the IKI Global Programme on Policy Advice for Climate Resilient Economic Development (CRED), implemented by Deutsche Gesellschaft für Internationale Zusammenarbeit (GIZ) GmbH on behalf of the German Federal Ministry for the Environment, Nature Conservation and Nuclear Safety (BMU).



On behalf of
German Federal Ministry for the Environment, Nature Conservation and Nuclear Safety (BMU)

Germany, 2021

# CONTENTS

# 1. INTRODUCTION

The objective of the Policy Advice for Climate – Resilient Economic Development (CRED) project is to develop tools to assess climatic risks in the partner countries as a consequence of the climate change, providing the necessary knowledge to design economic development strategies in consonance with the upcoming challenges in the medium and long term. Precisely, the project aims at generating country specific economic models that integrate the damage assessment, adaptation measures and inter – sectorial dynamics, in order to help the political decision makers to minimize the impacts and to design the necessary structural and economic measures.

The first stage of the economic models development required the generation of risk profiles for climatic hazards. In order to elaborate those risk profiles, it was necessary to evaluate the present characteristics and the future evolution of the climatic hazards using climate models. This analysis was performed under different greenhouse gases (GHG) scenarios and for different time horizons. The team in charge of the data collection and the analysis of the hazards evolution is the Sea Level and Climate Research team of the University of the Balearic Islands (UIB) (http://marine-climate.uib.es/).

The collection and data analysis process have been carried out according to the following stages:

i. *Selection of the models and simulations:* in this stage, the available simulations of the climate models whose domain included the countries of interest were retrieved from publicly accessible datasets. The files downloaded included all the variables necessary to characterize the hazards of interest.

ii. *Identification of climatic hazards*: in collaboration with local experts, the most relevant climatic hazards in terms of economic impact were identified using historical time series of hazard reports.

iii. *Definition of the climate hazard indicators*: once the most relevant hazards were identified, a set of indicators based on model data was define to characterize those hazards. The definition was carried out trying to keep the indicators as simple as possible while accurately representing the evolution of the hazards.

iv. *Data analysis and presentation of the results:* the last stage was the analysis of the hazards characteristics in the present climate and their projection for different time horizons along the 21st century. The results are summarized in maps, showing the spatial variability of the evolution of the hazards for different time horizons, and time series of the hazards yearly evolution at specific locations to be used in the economic models.

In this document, a detailed description of the methodology followed to complete each of these stages and the results of the analysis are presented.

# 2. MODELS AND SIMULATIONS

## 2.1 Functioning of the climate models

Climate models are computer programs that solve the mathematical equations that describe the transfer of energy and materials in the climate system. In particular, Global Climate Models (GCMs) characterize how energy and matter interact in different parts of the ocean, atmosphere, land, ice, etc., on a planetary scale. To do so, the models divide the Earth's surface into three-dimensional grid cells, solving the equations in each one of these cells at every time step (fig. 1). The size of the grid cells defines the resolution of the model: the smaller the size of the cells, the higher the level of detail in the model (resolution). Higher resolution models need more computing power to solve the equations, so a compromise has to be made between the desirable level of detail and the computing capacity available to run the model.

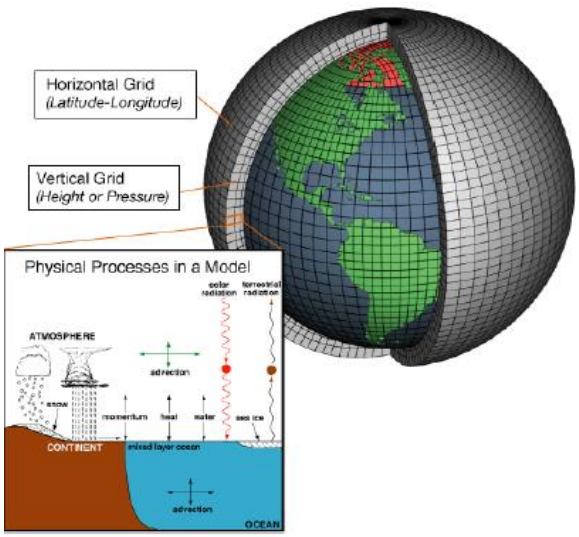


**Figure 1.** This figure shows the concept used in climate models. Each of the thousands of 3-dimensional grid cells can be represented by mathematical equations that describe the materials in it and the way energy moves through it. The advanced equations are based on the fundamental laws of physics, fluid motion, and chemistry. To "run" a model, scientists specify the climate forcing (for instance, setting variables to represent the amount of greenhouse gases in the atmosphere) and use powerful computers to solve the equations in each cell. Results from each grid cell are passed to neighboring cells, and the equations are solved again. Repeating the process through many time steps represents the passage of time. Image source: NOAA.

The GCMs resolution limits the range of climatic processes they can resolve. The resolution of the GCMs is at present typically of 50 km, meaning that they can accurately solve physical processes with characteristic length scales larger of twice that resolution. This can be a serious handicap when higher resolution is required to represent key aspects of the climate system like topographic elements. To overcome this limitation one solution is the implementation of Regional Climate Models (RCMs). As the name implies, a RCMs does not attempt to simulate the entire globe but only a portion thereof. They solve the same physical processes than the GCMs, using the same mathematical equations, but in a limited region. This spatial limitation means that the resolution can be increased, allowing the RCM to resolve regional or even local processes with accuracy. On the other hand, because they do not span the entire globe, RCMs must rely on information provided by GCMs at the lateral boundaries. In conclusion, regional models don't replace global models but are able to supply added value to simulations done with global models and to increase the number of climatic processes that can be faithfully resolved.

Once a climate model is set up, it can be run in different configurations. The most important one is known as "hindcasting." In this procedure, the model is run to simulate as accurately as possible the last decades. The model results are then compared against observations to so the scientists can check the accuracy of the model and, if needed, revise its equations and/or parameterizations. Research teams around the world test and compare their model outputs to observations and results from other models.

After the validation process, the climate models are assumed to be accurate enough for simulating future climate. To project the climate into the future, the model is configured as it was for the present climate, but some of the forcings are perturbed. Typically, the models are forced under different future scenarios. Scenarios are possible

evolutions of the GHG emissions to the atmosphere, which in turn will depend on how quickly human population will grow, how land will be used, how economies will evolve, etc... Climate scientists have agreed upon a set of scenarios that determine different levels of greenhouse gases in the atmosphere across the XXI century and beyond. One set of those scenarios is known as Representative Concentration Pathways or RCPs (IPCC et al., 2014). Each RCP indicates the amount of climate forcing, expressed in Watts per square meter, that would result from certain concentrations of greenhouse gases in the atmosphere These values are used to force the climate models projections in the future. There are four RCP scenario that are commonly used: RCP 2.6, which is the most optimistic, considers that all countries apply the restrictions agreed in the Paris Accords and drastically reduce the GHG emissions since the beginning of the 21st century. RCP 4.5 and RCP 6.5 are intermediate scenarios, which consider that the reduction of the GHG emissions begins in the decade of 2040 and the decade of 2060 respectively. Finally, RCP 8.5 scenario is the most pessimistic, considering that the GHG emission continues to grow in the 21st century at the same rate that it did along the 20th century (business as usual).

The standard protocol for a study of the climate evolution using a climate model is to perform three different type of simulations: historical, projection and control. The historical simulation reproduces the climate of the industrial period, usually spanning from the start of the Industrial Revolution (mid XIX century) to the beginning of the 21st century. It is important to point out that the historical simulations are free runs, meaning that the model is not constrained by the assimilation of any observational data. This means that the chronology of the climatic events does not follow the actual chronology of the past climate. The historical simulations reproduce the mean values, interannual and seasonal variability and multi-decadal trends accurately, but not specific events at a particular date. The same applies to the projection runs, which simulate the climate evolution along the 21st century under a specific RCP scenario, staring at the end of the historical run. The same historical run is usually used as the starting point of several projection runs under different scenarios of GHG emissions. Finally, the control run is a simulation of the future climate in which no change in the GHG is considered. By comparing the control run and the projections one can separate out any trends in the model outputs that are due to numerical drifts in the model (i.e. captured by the control run) and the trends caused by the changes in the GHG concentrations (projections run). The evolution of the climate in the future under the different emission scenarios is assessed by comparing the historical and projection runs.

## 2.2 Global simulations

The most extensive public dataset of state-of-the-art global climate models is the one generated in the frame of the different phases of the Coupled Model Intercomparison Projects (https://www.wcrp-climate.org/wgcm-cmip/ , the most used right now is the 5th phase and the 6th phase is upcoming). The CMIP projects are an international initiative that gathers modeling groups from many institutions around the world. Its main objective is to generate a large ensemble of coordinated global climatic simulations based on coupled atmosphere – ocean models with similar characteristics that allow model intercomparison and climate change analysis. Each simulation is run independently by the different modeling group using different models and parameterizations. This allows an adequate characterization of uncertainties linked to model choice, natural variability and scenario selection. The simulations data is available in several servers, and can be downloaded after registration. For instance, at the Earth System Grid Federation (ESFG) node at German Climatic Centre (DKRZ) (https://esgf-data.dkrz.de/projects/esgf-dkrz/).

The development of the economic models of the CRED project requires the evaluation of the climatic hazards evolution at country scale. For this purpose, the CMIP global models are not ideal due to their low resolution, which limits their capacity to resolve regional scale processes. For this reason, the analysis has been carried out using RCM simulations. Nonetheless, the methodology described in the following sections can be applied to GCMs if needed to complete a more general picture of the climate evolution in a wider region.

## 2.3 Regional simulations

The RCM simulations analyzed in this study are part of the CORDEX dataset (https://cordex.org/). CORDEX is an initiative of the World Climate Research Program (WCRP) devoted to the development, evaluation and exploitation of RCM in different regions of the world. These experiments are carried out by independent research groups, using different numerical codes, but with standardized configurations and regional domains. This allows the intercomparison of the simulations and the analysis of large ensembles of experiments, increasing the robustness of the climatic projections. CORDEX simulations were considered the best option to fulfill the objectives of the project due to its high resolution and the fact that they will be used in the next IPCC (Intergovernmental Panel for Climate Change) reports. Among the CORDEX domains, the Central Asia domain (CAS) is the only one including Georgia (fig. 2).

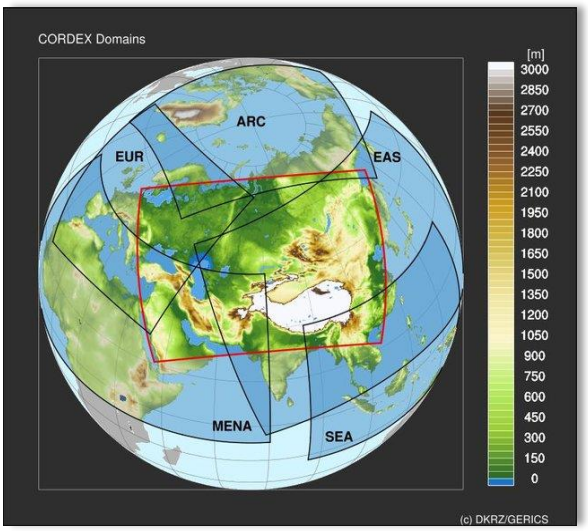


**Figure 2.** Boundaries of some of the regional CORDEX domains. The Central Asia domain (CAS) is marked in red.

The simulations and variables selected from the CORDEX dataset are summarized in table 1. A total of 12 simulations carried out by two different RCMs forced by 4 different GCM has been used. For each RCM-GCM combination available, historical and projection runs for RCP 2.6 and RCP 8.5 scenarios were downloaded. The selection and downloading processes will be detailed in the following section.

The two RCMs used on the selected simulations are the GERICS-REMO2015 model (Jacob, 2001; Jacob et al., 2012) and the ALARO-0 model (Gerard et al., 2009; Giot et al., 2016). Both models have successfully being used in previous climate studies on other CORDEX domains (De Troch et al., 2013; Giot et al., 2016; Hamdi et al., 2012; Pietikäinen et al., 2018; Termonia et al., 2018). The simulations on the CAS domain used here are very recent, performed between 2019 and 2020, so there are still no climatic studies analyzing them in the literature. Nonetheless, Top et al. (2020) carried out and exhaustive validation study of the two models in the CAS domain. The authors compared the results of two simulations (one for each model), forced by the ERA-Interim reanalysis, with an extensive dataset of gridded temperature and precipitation products, based on both reanalysis and observations. Although the results showed some bias in the daily temperature range and the seasonality of the precipitation, the authors conclude that GERICS-REMO2015 and ALARO-0 RCMs can be used to perform projections over Central Asia and that the produced climate data can be applied in impact modelling. Regarding the objectives of the CRED project, the results of Top et al. (2020) support that the simulations analyzed are based on accurate RCMs and hence the results obtained for the evolution of the climatic hazard are reliable and robust.

| RCM | ALARO-0 | GERICS-REMO2015 | | |
|---|---|---|---|---|
| Driving GCM | CNRM-CERFACS-CNRM-CM5 | MOHC-HadGEM2-ES | MPI-M-MPI-ESM-LR | NCC-NorESM1-M |
| Variables | Precipitation<br>Temperature | Precipitation<br>Temperature<br>Max Wind Speed<br>Relative humidity | Precipitation<br>Temperature<br>Max Wind Speed<br>Relative humidity | Precipitation<br>Temperature<br>Max Wind Speed<br>Relative humidity |
| Frequency | Daily | Daily | Daily | Daily |
| Spatial resolution | 0.22° (~25 km) | 0.22° (~25 km) | 0.22° (~25 km) | 0.22° (~25 km) |
| Runs<br>Historical<br>(1970 -2005)<br>RCP 2.6<br>(2006 – 2100)<br>RCP 8.5<br>(2006 – 2100) | ALARO-CNRM-HIST<br>ALARO-CNRM-2.6<br>ALARO-CNRM-8.5 | REMO-MOHC-HIST<br>REMO-MOHC-2.6<br>REMO-MOHC-8.5 | REMO-MPI-HIST<br>REMO-MPI-2.6<br>REMO-MPI-8.5 | REMO-NCC-HIST<br>REMO-NCC-2.6<br>REMO-NCC-8.5 |

**Table 1.** Summary of the simulations and variables used in the study.

## 2.4 RCM data selection and downloading

The CORDEX (and CMIP) data are hosted in several severs located at different institutions around the world. The Earth System Grid Federation (ESFG) is a platform that allows the access to the different nodes (servers). In our case, we have used the German Climatic Centre (DKRZ) node (https://esgf-data.dkrz.de/projects/esgf-dkrz/). The reason of choosing this node is that the simulations used in the study are hosted in this server and the downloading was faster. Nevertheless, using another node wouldn't be a problem, as all the simulations hosted in any server can be accessed from all the nodes.

The data are public and available for any user. The downloading process follows the next steps:

1. Registration on the node website (https://esgf-data.dkrz.de/projects/esgf-dkrz/). Once the registration form is completed the user will be assigned an OpenID, a username and a password. With these credentials the user can access the search engine.

2. After accessing the search engine of the platform (https://esgf-data.dkrz.de/search/cordex-dkrz/), the user can navigate through the menu to select the different products. In the case of this study, the selection was:

   - Domain: CAS-22
   - Experiment: historical, rcp26 and rcp85
   - Time Frequency: day
   - Variable: pr, tas, srfWindmax and hurs
   - Variable Long Name: Precipitation, Near-Surface Air Temperature, Daily Maximum Near-Surface Wind Speed, Near-Surface Relative Humidity.

Note, that to select the variable, it is enough to indicate either the short or the long name, it is not

necessary to mark both of them. There is no need to set any of the other fields (project, product, institute, etc.). Figure 3 shows an example of a search for historical runs of daily precipitation in the CAS domain.

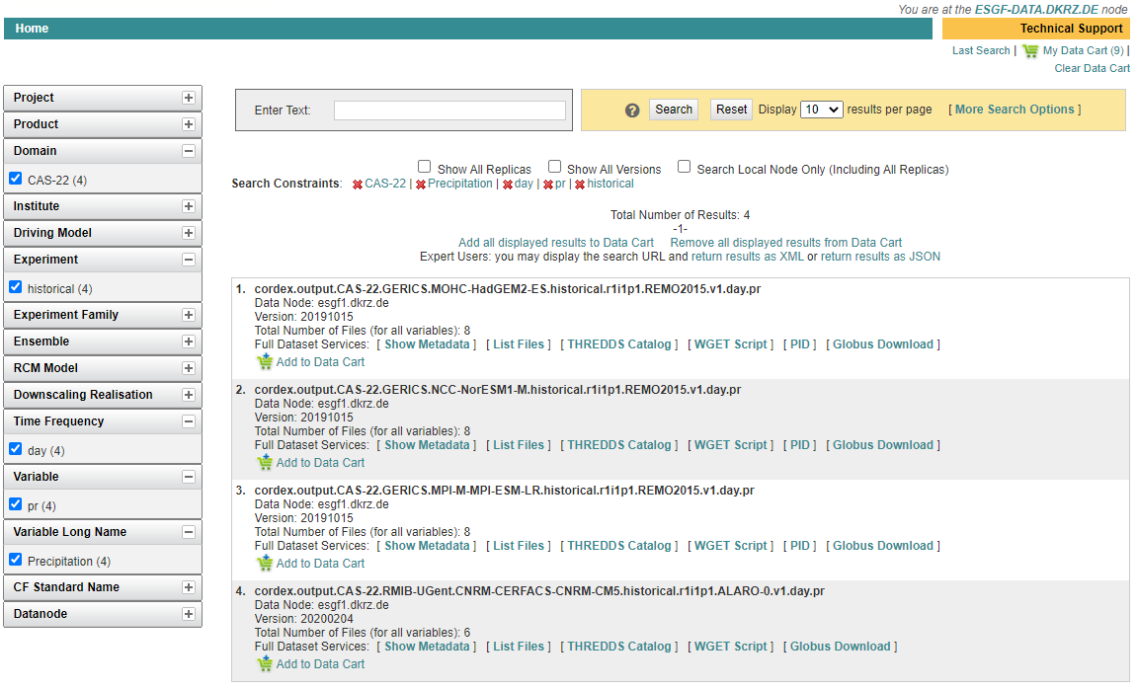


**Figure 3.** Results for historical runs of precipitation daily data in the CAS CODEX domain.

3. The results of the example of figure 3 shows how the search results are displayed. Each of the 4 results correspond to the historical daily outputs of the four simulations available (table 1). Each set of outputs is comprised by a number of files that fluctuates depending on the simulation and temporal resolution. By clicking on 'list files' the individual files are shown. The file naming is standardized for all CORDEX simulations as follows:

VariableName_Domain_GCMModelName_CMIP5ExperimentName_CMIP5EnsembleMember_
RCMModelName_RCMVersionID_Frequency_StartTime-EndTime.nc
Example:
pr_CAS-22_NCC-NorESM1-M_historical_r1i1p1_GERICS-REMO2015_v1_day_19960101-20001231.nc
VariableName: pr (precipitation)
Domain: CAS-22 (Central Asia 0.22° resolution)
GCMModelName: NCC-NorESM1-M (forcing CMIP5 GCM)
CMIP5ExperimentName: historical (run type)
CMIP5EnsembleMember: r1i1p1 (identification of the CMIP5 run)
RCMModelName: GERICS-REMO2015 (RCM used in the domain)
RCMVersionID: v1 (version of the RCM)
Frequency: day (temporal frequency)
StartTime-EndTime: 19960101 – 20001231 (data period in the file; yyyymmdd)

Figure 4 shows the unfolded file list for the first set of data outputs of figure 3, corresponding to the historical daily precipitation of the REMO simulation forced by MOHC-HadGEM2-ES (REMO-MOHC-HIST, table 1).

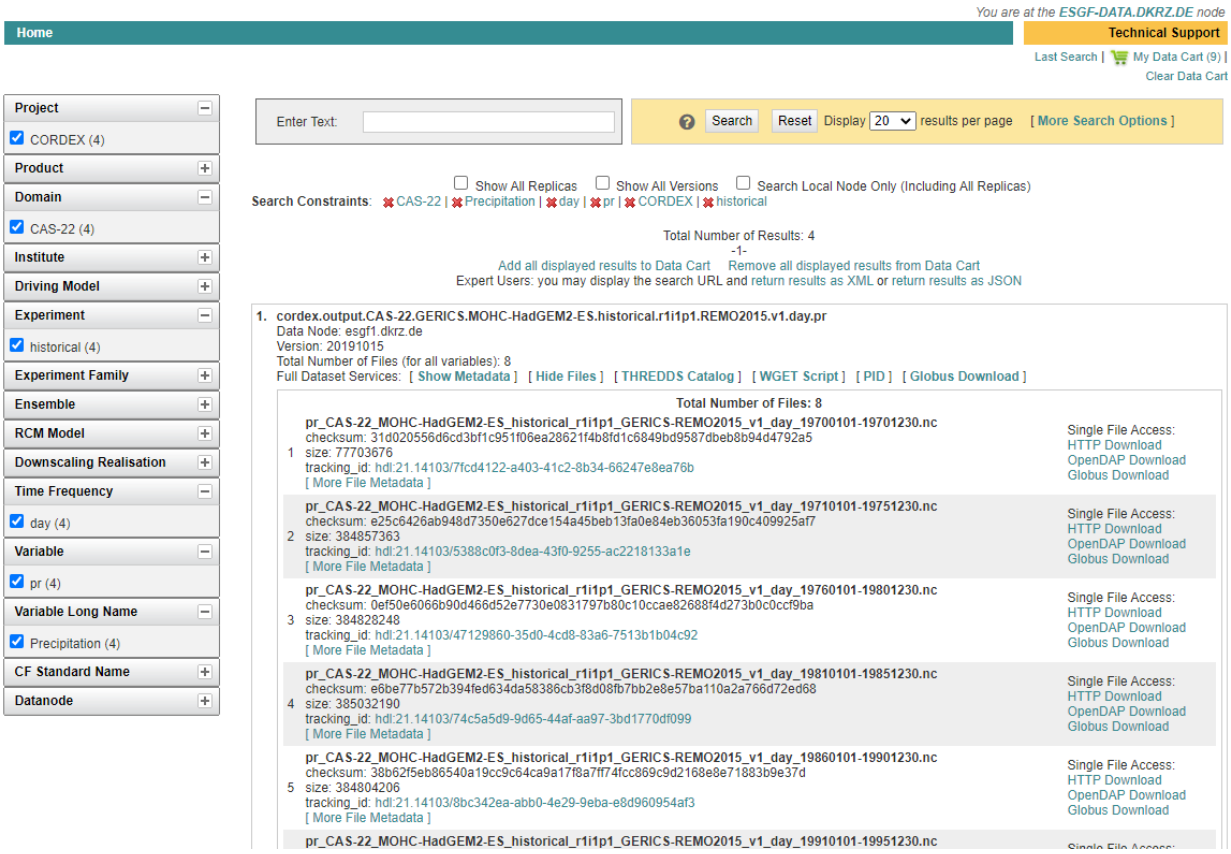


**Figure 4.** Unfolded files of the first set of models outputs in figure 2.

4. Individual files can be directly downloaded by clicking on 'HTTP download' (fig. 4). However, a faster and more convenient way of retrieving the data is by downloading all the datasets automatically. This can be done using a Linux script generated by the server. To do so, first the datasets have to be added to the data cart by clicking on 'Add to Data Cart' (fig. 3). Once all the datasets are selected, by clicking on 'My data Cart' the selection will be shown (fig. 5). By ticking 'select all datasets', they will be all selected (if only some of the datasets are required, the selection can be done manually). Finally, by clicking on 'WGET Script '(fig. 5), a BASH script will be generated with the specific code to download all the selected data.

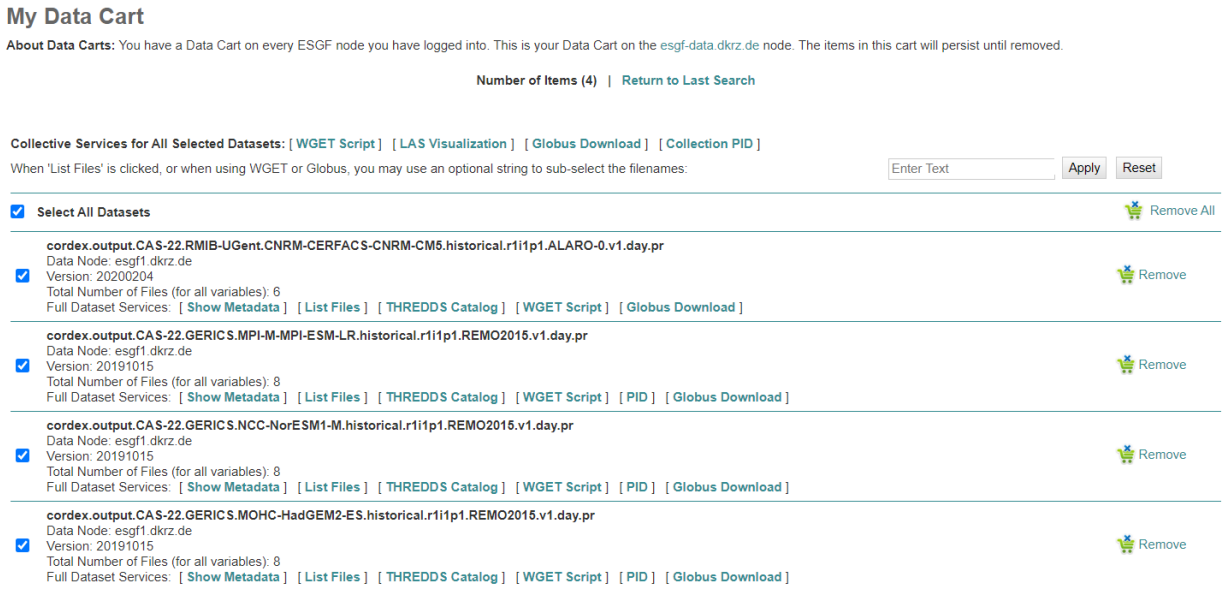


**Figure 5.** Example of the Data Cart with the selection of all the datasets searched in figure 2.

5. The script should be run in the directory where the files are to be stored. After assigning the correct permissions, by typing './ScriptName.sh –help' in the Linux terminal the running options will be listed. The easier and most direct option is by introducing manually the user's CORDEX credentials, using the option ' ./ScriptName.sh –H' ' (fig. 6). This will start the automatic download of all the files from all the selected datasets included in the script. While running, the script will also show the progress of the process. If there is an error downloading any specific file it can be downloaded later manually or by generating another script. Once the script has finished all the files of the selected datasets will appear in the running folder.

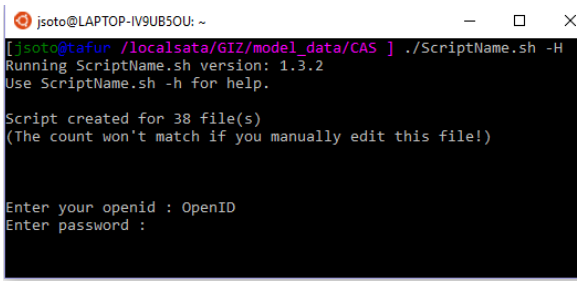


**Figure 6.** Example of how to run the BASH script for the automatic files download.

## 2.5 Files reading

The models output files are given in the Network Common Data Format (netCDF, with the extension '.nc'). NetCDF is the most extended format for data storage in the modeling community because it allows the storage of arrays and matrices in a self-explanatory way. It also allows the partial access to the data, which is very useful considering the large amount of information usually contained in a single file.

The structure of the files includes the grid (domain), spatial dimensions (longitude and latitude) and the temporal dimension (time) of the period included in the file. The climatic variables are stored in the form of 3D-matrices with dimensions: longitude x latitude x time. The information of the grid characteristics, the origin of the time counter and the variable properties are included in the metadata of the file. The model developers can include multitude of attributes of the variables in the file metadata to clarify their properties (dimensions, names, units, etc.). Information about the model and simulation specifications (institution, GCM, RCM, etc.) is usually also added as the general attributes of the files. Reading the metadata is very useful and easy with any of the common netCDF reading tools. There are plenty of free available data processing tools to manage netCDF files. A summary of the most commonly used can be consulted in the users

portal of the DKRZ (https://www.dkrz.de/up/services/analysis/data-processing/tools). In this study, all the data processing has been carried out using MATLAB software, which includes netCDF processing tools.

CAS is one of the CORDEX larger domains. It extends approximately between 11° E and 140° E in longitude and between 18° N and 60° N in latitude (the limits might be slightly different depending on the specific RCM grid). This extension results in very large netCDF files for each of the model fields, including information about regions not relevant for this study. Processing such large files could generate storage and computation capacity problems. To avoid these problems, a subset of the files data including the Georgia region was selected, thus reducing the size of the information processed. The limits of this subset are:

- Longitude: [39.5° E – 47° E]
- Latitude; [41° N – 43.8° N]

The selection of a subset of data is quite simple using any of the aforementioned netCDF data processing tools. All the computation procedures described in the following sections were carried out using the subset of the model fields within these limits.

# 3. CLIMATE HAZARDS AND INDICATORS

The selection of the climatic hazards to be analyzed was carried out in collaboration with the local partners, who provided historical data of climatic hazards with substantial impacts in the country (i.e. loss of human lives, impacts on infrastructures, economic losses). During several meetings with the local partners the most relevant hazards were identified. A key point in this process was the evaluation of the capacity of the models to properly characterize those events. After considering several possibilities, the agreement was to focus on six different climatic hazards: extreme precipitation, extreme temperature, extreme wind events, heatwaves, droughts and wildfires. Then, a set of indicators was defined to characterize and quantify those hazards in the present and future climate. Those indicators can be classified in two types:

- Extreme events: defined as the number of days the value of the variable characterizing the hazard is above the 99th quantile computed from the historical period. These indicators were defined for the precipitation, temperature and maximum wind speed. For the heatwaves, a combination of extreme temperature and duration is applied in the indicator definition.
- Empirical indices: indicators specifically designed to describe a rather complex hazard that depends on several climatic variables. This kind of indicators were used in the characterization of the droughts and wildfires. Values of the index over a given threshold imply high risk of a hazardous event.

Table 2 summarizes the hazards and their correspondent indicator.

| Hazards | Indicator |
|---|---|
| Extreme Precipitation | Days with P › q99 |
| Extreme Temperature | Days with T › q99 |
| Extreme Wind | Days with max W speed › q99 |
| Heatwaves | 5 or more days with T › q99 |
| Droughts | SPEI Index ‹ -2 |
| Wildfires | KBDI Index › 150 |

**Table 2.** Summary of the hazards and the indicators defined for each one of them.

## 3.1 Extreme events

Extreme events indicators were defined for the daily temperature, precipitation and maximum wind speed. They are computed as the number of days per year that a variable exceeds the 99$^{th}$ quantile of the historical period. The historical period is defined as the 30-year period of each historical simulation before the projection starts, i.e. between 1976 and 2005 (projection runs start in 2006; table 1). The 99$^{th}$ quantile corresponds to the threshold below which 99% of the data is found. In other words, it determines the limit above which the highest 1% of the values over the historical period are found.

Figure 7 illustrates an example of how the evolution of the extreme temperature is characterized at the model grid point close to Almay. The historical period is represented in blue and the RCP 8.5 projection in green. The black horizontal line marks the threshold of the q99 of the historical period. The yellow points are the temperature extreme events over this threshold in the historical period while the orange points are the events over the threshold in the projection. A way to summarize this result is to compute the difference between the number of days per year over the threshold in the future (orange points) and present (yellow points). The three vertical red lines divide the projection into three 30-year periods: beginning of the century (2011 – 2040), midcentury (2041 – 2070) and end of the century (2071 – 2100). These periods are used as reference to evaluate the hazards evolution (see section 4).

The same methodology described in the example is applied to all the hazard indicators, except for the heatwaves, for which two complementary magnitudes are defined and evaluated.

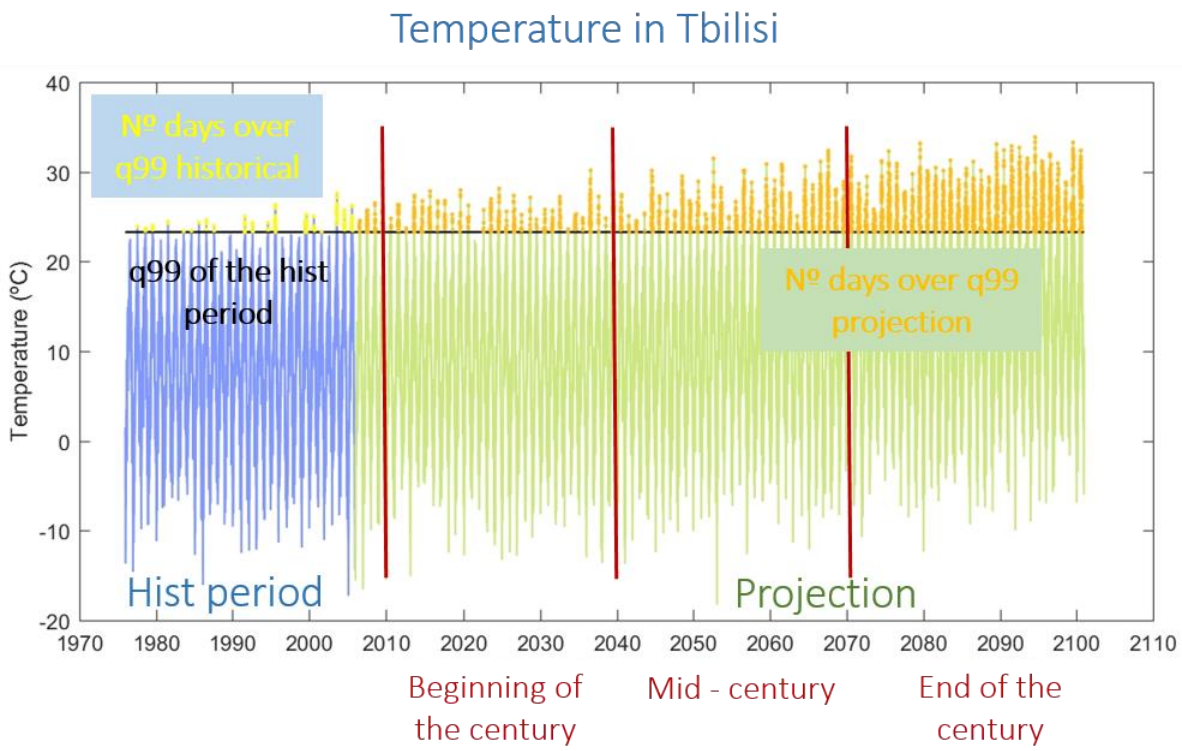


**Figure 7.** Time series of the temperature in the grid point closer to Almaty. The blue line corresponds to the historical period and the green line to the RCP 8.5 projection. The black horizontal line is the q99 threshold of the historical period. Yellow points indicate the values of extreme temperature over the historical period and orange points over the projection. The three vertical red lines mark the limits of the three time horizons considered: beginning of the century (2011-2040), midcentury (2041-2070) and end of the century (2071-2100).

## 3.2 Heatwaves indicators

Heatwaves are a special case of extreme events. They are defined as the occurrence of extreme temperature prolonged over time. There are plenty of definitions for the heatwaves in the literature, which differ on the temperature threshold and the minimum length considered to characterize an event as a heatwave (Xu et al., 2016). In this study we have adopted the following definition: a heatwave occurs when extreme temperatures, over 99th quantile of the historical period, are prolonged during a period of at least five days. Using this definition, the heatwave in the historical and projection periods were identified and characterized.

Three magnitudes are defined to characterize a heatwave: occurrence, duration and intensity.

- The occurrence is used to compute the number of heatwaves in the different periods, in the same way that the rest of the extreme events are counted.
- The duration is the number of consecutive days that temperatures exceed the threshold. The minimum duration is 5 days by definition.
- The intensity is defined by the following equation:

$$I = \int_{t0}^{t1} (T - Tthr)dt \quad (1)$$

Where $t_{0/1}$ are the time at the beginning and end of the heatwave, $T$ is the temperature and $T_{thr}$ is the temperature threshold (q99th of the historical period). The intensity measures the severity of a specific heatwave. The higher the temperatures reached and the longer the duration the more intense the heatwave.

These three magnitudes are used as the indicators to characterize the heatwaves in the present and future climate. In other words, for the heatwaves, not only the change in the number of events per year will be evaluated, but also the evolution of the duration and intensity of those events.

## 3.3 Droughts indicator

The indicator used for the analysis of the droughts is the Standardized Precipitation Evapotranspiration Index (SPEI) (Vicente-Serrano et al., 2010). The SPEI is based on precipitation, temperature and humidity data, and it has the advantage of combining multi-scalar character (can be calculated using different temporal windows) with the capacity to include the effects of temperature variability on drought assessment. The procedure to calculate the index involves a climatic water balance, the accumulation of deficit/surplus at different time scales, and adjustment to a log-logistic probability distribution. A complete summary of the index properties and its advantages with respect to other indicators can be consulted in the cited reference and in the website https://spei.csic.es/, which gathers multitude of studies about the index validation and a global SPEI gridded dataset. A toolbox for the computation of the SPEI on R can be also downloaded from that website.

In this study the SPEI have been computed using the Climate Data Toolbox for MATLAB (Greene et al., 2019), which includes specific functions to calculate the index. Besides details about the characteristics of the region of study (geographical coordinates, solar radiation), the SPEI computation uses monthly temperature and precipitation fields. Therefore, the daily model outputs were monthly averaged before the computation. According to the SPEI values, the conditions of the region analyzed can be classified in five drought classes (Paulo et al., 2012): non-drought (SPEI > -0.5), ‚mild ( -1 < SPEI < -0.5), moderate (-1.5 < SPEI < -1), severe (-2 < SPEI < -1.5), and extreme (SPEI < -2).

The droughts events in this study have been defined as those included in the extreme classification, i.e. those events for which the SPEI is lower than -2. Using this criterion, the droughts events where identified in the historical and projection runs, and their evolution estimated as the increase/decrease of the number of events per year between the future and the present climates.

## 3.4 Wildfires indicator

Although many factors, both natural and anthropogenic, are determinant in forest fires, daily weather conditions have been found to be especially important (Bessie and Johnson, 1995). Accordingly, strong efforts have been devoted to analyze how to predict the fire ignition and behavior. The research has been focused on describing fire weather conditions, and integrating different meteorological variables into fire indices. These efforts resulted in a wide array of fire danger rating systems and indices that can be used to assess wildfires hazards. These various fire indices differ in many aspects. Some of them not only include relationships between weather conditions and fire activity but also between fire activity and soil moisture and fuel properties. For instance, some very simple indices intending to assess fire ignition probability only consider day-to-day weather conditions. Other more complex indices are cumulative and consider water content in soil or fuels over longer periods, being thus suitable for predicting fire intensity or spread. A thorough summary of the most used fire indices and reference studies can be consulted at https://wikifire.wsl.ch/.

In order to select a suitable wildfire index, a compromise had to be made between the index complexity and the climatic variables available. This led to the selection of the Keetch-Bryan Drought Index (KBDI) (Keetch and Byram, 1968). The KBDI have been satisfactorily used in wildfire projection studies when other more complex indices cannot be computed (Brown et al., 2020).

The KBDI is calculated using daily maximum temperature, daily precipitation, and annual accumulated precipitation (Keetch and Byram, 1968). As a substitute for fuel availability in an area, the KBDI uses cumulative annual precipitation and assumes that higher annual rainfall corresponds to more vegetation, and therefore more fuel available

to burn. The KBDI formula approximates the amount of evapotranspiration as a proxy to account for the dryness of the upper soil layers and the flammability of organic matter. The calculated KBDIs fall within a range from 0 to 203.2, which is equivalent to the amount of water necessary (in mm) to bring the soil up to an assumed complete saturation of 0.2 m. For example, a KBDI value of 0 indicates that the soil is completely saturated, and the potential of a wildfire is low; whereas a KBDI value of 203.2 indicates extreme drought and fire risk. The KBDI is calculated on a daily basis, following the equations (Alexander, 1990):

$$KBDI_t = Q + \frac{(203.2-Q)\cdot\left(0.968\cdot e^{0.0875\cdot T+1.5552}-8.30\right)\cdot\Delta t}{1+10.88\cdot e^{-0.00174\cdot P}}\cdot 10^{-3} \quad (2)$$

$$Q = KBDI_{t-1} - P_{net} \quad (3)$$

$$P_{net} = \max(0, P_t - 5.1) \quad (4)$$

Where $KBDI_t$ is the index in the time $t$, $Q$ is moisture deficit (in mm), $T$ is the daily maximum temperature (in °C) and $P$ the mean annual precipitation (in mm). $Q$ is calculated by subtracting the net precipitation, $P_{net}$, to the index value in the previous time step, $KBDI_{t-1}$. The net precipitation is estimated as the maximum between 0 and the difference between the precipitation in the time $t$, $P_t$, and 5.1 (in mm).

Since the index computation is recursive, it needs to be initialized. Ideally, KBDI could be set to zero after a period of 15.24−20.32 cm of precipitation or more accumulated in one week. However, this requirement is difficult to meet in the very dry regions of the area of study. Therefore, an initialization procedure has to be performed (Brown et al., 2020). First, we have identified the week of maximum precipitation for the first year of data and set the KBDI to zero for that week. Using it as an initial point, KBDI is calculated on the basis of the KBDI value from the previous day. During the initialization (or spin-up) stage of KBDI, the first-year data is used in a loop to repeat the daily KBDI calculations. When the differences between the daily KBDIs calculated in loop (n) and loop (n-1) are smaller than a threshold, in our case 8 mm, the daily KBDIs are considered as stable as being the closest to the 'real' KBDIs of the first year. At this point, the initialization of KBDI is completed. The KBDI on the last day of the first year, which is calculated in the loop (n), is then used to estimate the KBDI on the first day of next year, and so forth so on for the subsequent time periods.

The KBDI values between 150 and 200 correspond to severe dry conditions and extreme fire risk (Keetch and Byram, 1968). Once the index has been calculated at each grid point for the historical and projection runs of all the simulations, the extreme fire risk events are computed as the days with KBDI higher than 150. Using this criterion, the evolution of the wildfire hazards between the present and future climates is estimated as the increase/decrease of the number of events between the future and the present climates.

## 3.5 Ensemble average and spread

The hazard indicators were computed for all the simulations following the methodology described. According to the variables available for each model (table 1), for the ALARO-0 simulations the indicators for extreme winds and droughts (SPEI) events could not be calculated because the wind speed and the relative humidity were not available. For the GERICS-REMO2015 simulations all the indicators were computed. As a result, an ensemble with information of the hazards characteristics was generated, comprised by 4 or 3 historical simulations and 8 or 6 projections simulations (one for each RCP scenario, 2.6 and 8.5) for each indicator.

To integrate the information from the different simulations, the final results of the hazards evolution are presented using the ensemble average. The results of all the historical simulations and the projections under the same RCP scenarios for each hazard are averaged, and this average is considered the most accurate representation of present and future hazards. To provide an estimation of the accuracy of the ensemble average, the uncertainty of the projection for each scenario is defined as the fraction between the ensemble spread (difference between the higher and lower values among the projections of the different simulations) divided by the ensemble average. By definition, if the spread is smaller than the average of the ensemble the uncertainty will be lower than 1 and the results for that indicator can be considered robust. Conversely, if the spread is higher than the ensemble average, the uncertainty will be higher than 1 and the results are less robust. This methodology is commonly used in the climatic studies to provide information about the agreement among models.

# 4. RESULTS

The information about the present characteristics and future evolution of the hazards over the whole country have been integrated in figures and time series. Two types of figures have been produced and are included in the Appendix A. The first type represents the characteristics of the hazards in the present climate and the uncertainty of the spread. The second type shows the future evolution of the hazards. For each indicator the information summarized in the figures and the time series are the following:

- A figure with three panels. In the top panel a map with the values defining the hazard in the present climate is presented (see fig. 8 as an example). The present climate or historical period is 1976 – 2005. The maps show the 99th percentile for the precipitation, temperature and maximum wind speed. For the heatwaves, maps for the average number of events per year, intensity and duration in the present climate are provided. For the SPEI and KBDI, maps of the average number of events per year are represented. In the second and third panel, the maps with the ensemble uncertainty for the RCP 2.6 and RCP 8.5 scenario projections are included.

*Example of the present climate and model uncertainty figures*

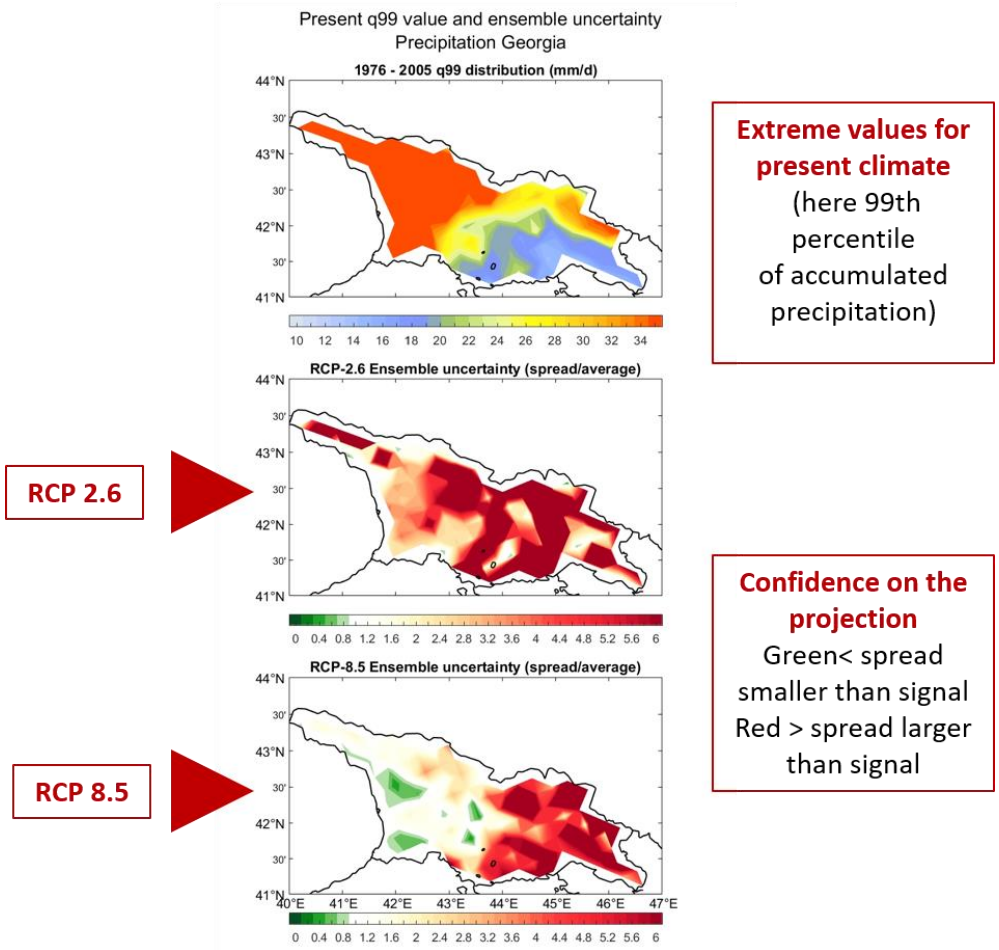


**Figure 8.** Example of the maps summarizing the present climate and model uncertainty. The top panel shows the average extreme precipitation values in the historical period. The central and bottom panels the ensemble uncertainty for the RCP 2.6 and RCP 8.5 scenarios, respectively.

- A figure with maps representing the time evolution of all the indicators (see fig. 9 as an example). This is done under RCP 8.5 and RCP 2.6 emission scenario with respect to the historical period (1976 – 2005) for three 30 – year time horizons: beginning of the 21st century (2011 – 2040), mid – 21st century (2041 – 2070) and end of the 21st century (2071 – 2100) (see fig. 7). These maps show the increase/decrease of the indicators with respect to the historical period in number of events per year or percentage, depending on the indicator (for some indicators, such as the heatwaves, the number of events in the present is cero, so is not possible to express the increase in percentage). For the heatwaves the increase/decrease of the duration and intensity is also given.

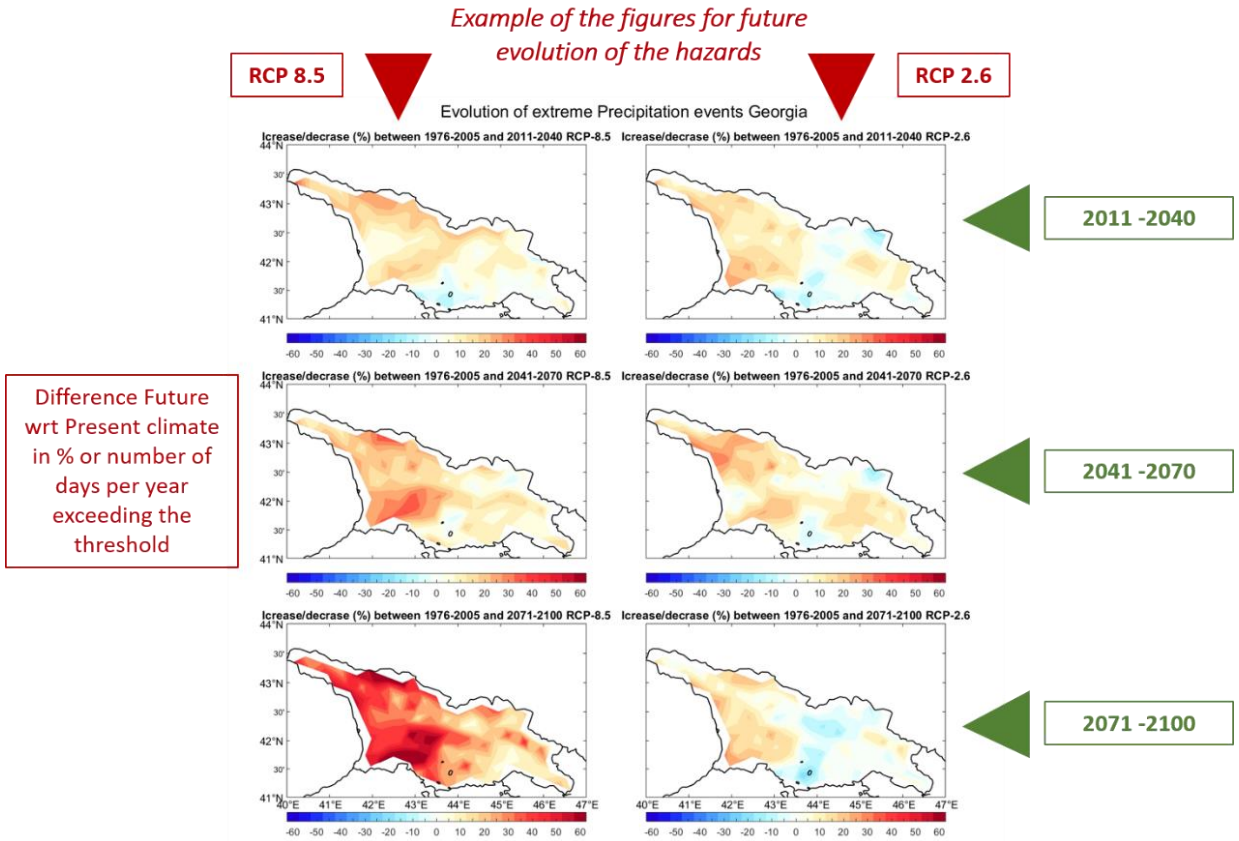


**Figure 9.** Example of the maps summarizing the time evolution of the extreme precipitation events in the 21st century. The left panels show the evolution under RCP 8.5 scenario and the right panels under RCP 2.6 scenario. The top panels show the average increase/decrease (in %) of the number of events per year with respect to the historical period by the beginning of the century, the center panels by midcentury and the bottom panels by the end on the century.

- Yearly time series of all the indicators in excel format for specific locations. Instead of providing directly the model outputs, we provide a smoothed version which is more convenient for the economic models. Namely, the time series are produced by adjusting a second degree polynomial to the average number of events per year of the indicators for the historical period and the three projection time horizons (fig. 10). A map with the location of the cities/regions where the series are computed and the values of the thresholds at these locations are also included in the files (fig. 11).

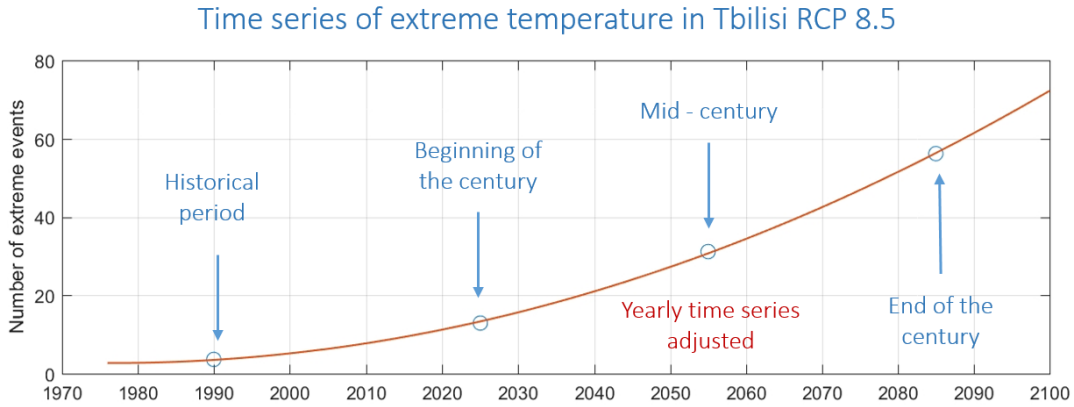


**Figure 10.** Example of how the yearly time series of the extreme temperature in Almaty is computed for the RCP 8.5 projection. The blue circles represent the average of the number of events per year for the historical period and the three time horizons defined for the 21st century. The red line is the time series resulting of adjusting the four 30-year averages to a second degree polynomial function.

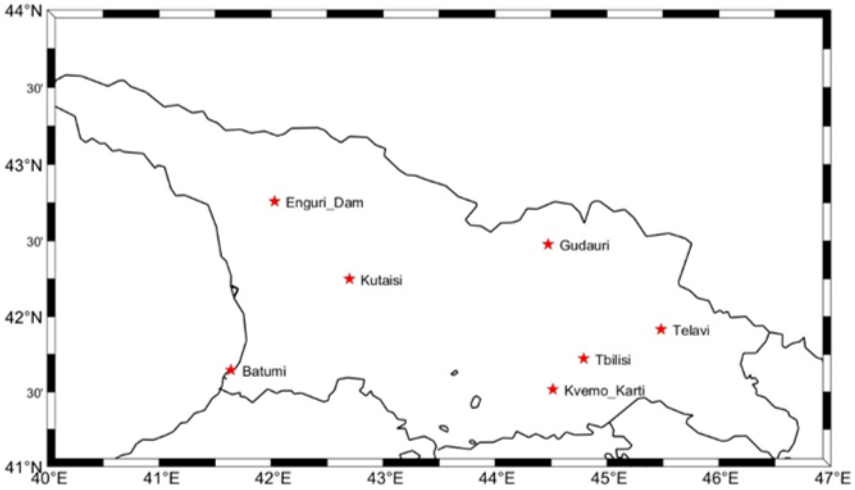


**Figure 11.** Locations of the point/regions where the yearly time series of the indicators are computed.

The figures and time series files included in the dataset for Georgia are summarized in table 3.

**Table 3.** Figures and time series files for each partner country included in the dataset.

| Hazards | Georgia |
|---|---|
| Extreme Precipitation | 2 figures files (jpg format)<br>1 excel file with 2 time series |
| Extreme Temperature | 2 figures files (jpg format)<br>1 excel file with 2 time series |
| Extreme Wind | 2 figures files (jpg format)<br>1 excel file with 2 time series |
| Heatwaves | 6 figures files (jpg format)<br>1 excel file with 2 time series |
| Droughts | 2 figures files (jpg format)<br>1 excel file with 2 time series |
| Wildfires | 2 figures files (jpg format)<br>1 excel file with 2 time series |
| Total files | 22 files |

The figures for all the indicators (table 3) are shown in Appendix A. Also, all the figures and the excel files with the time series are available at the on-line repository https://zenodo.org/record/4506374#.YEdhHp1KhPZ (doi: 10.5281/zenodo.4506374).

In addition, netCDF files with the yearly time evolution of all the indicators have been generated and stored in the same repository. The files contain 3D matrices (dimensions: longitude x latitude x time), and include the total number of events for each hazard on each year between 1976 and 2100. For the heatwaves, the files also include the yearly averaged intensity and duration. The files were generated for the complete CORDEX CAS domain. One file was generated for each hazard, each simulation and each emission scenario, resulting in a total of 44 files. Following the netCDF convention, the files include the information on the content.

Table 4 summarizes the files generated for each indicator. The files naming format is the following:

VariableName_Domain_GCMModel_ RCPscenario_RCMModel_Frequency_StartTime-EndTime.nc

Example:

xtrmpr_CAS-22_NCC-NorESM1-M_rcp26_GERICS-REMO2015_yr_1976-2100.nc

VariableName: xtrmpr (extreme precipitation)
Domain: CAS-22 (Central Asia 0.22° resolution)
GCMModel: NCC-NorESM1-M (forcing CMIP5 GCM)
RCPscenario: rcp26 (historical + projection)
RCMModel: GERICS-REMO2015 (RCM used in the domain)
Frequency: yr (yearly temporal frequency)
StartTime-EndTime: 1976 – 2100 (data period in the file; yyyy)

| Hazards | Variable Name in file | Number of files | |
|---|---|---|---|
| Extreme precipitation | xtrmpr | 4 simulations<br>2 RCP scenario | 8 |
| Extreme Temperature | xtrmtemp | 4 simulations<br>2 RCP scenario | 8 |
| Extreme Wind | xtrmwnd | 3 simulations<br>2 RCP scenario | 6 |
| Heatwaves | hw | 4 simulations<br>2 RCP scenario | 8 |
| Droughts | drght_risk | 3 simulations<br>2 RCP scenario | 6 |
| Wildfires | wildfr_risk | 4 simulations<br>2 RCP scenario | 8 |
| | | Total files | 44 files |

**Table 4.** Summary of the variables and files generated for each hazard.

**Dataset Citation:** Soto-Navarro, Javier, & Jordá, Gabriel. (2021). Policy Advice for Climate – Resilient Economic Development (CRED) project central Asia climatic hazards database [Data set]. Zenodo. http://doi.org/10.5281/zenodo.4506374.

# REFERENCES

Alexander, M.E., 1990. Computer Calculation of the Keetch-Byram Drought Index-Programmers Beware! Fire Manag. Notes 51, 23–25.

Bessie, W., Johnson, E., 1995. The Relative Importance of Fuels and Weather on Fire Behavior in Subalpine Forests Author ( s ): W . C . Bessie and E . A . Johnson Published by : Wiley Stable URL : http://www.jstor.org/stable/1939341 REFERENCES Linked references are available on JSTOR f. Ecology 76, 747–762.

Brown, E.K., Wang, J., Feng, Y., 2020. U.S. wildfire potential: a historical view and future projection using high-resolution climate data. Environ. Res. Lett. https://doi.org/https://doi.org/10.1088/1748-9326/aba868

De Troch, R., Hamdi, R., Van de Vyver, H., Geleyn, J.F., Termonia, P., 2013. Multiscale performance of the ALARO-0 model for simulating extreme summer precipitation climatology in Belgium. J. Clim. 26, 8895–8915. https://doi.org/10.1175/JCLI-D-12-00844.1

Gerard, L., Piriou, J.M., Brožková, R., Geleyn, J.F., Banciu, D., 2009. Cloud and precipitation parameterization in a meso-gamma-scale operational weather prediction model. Mon. Weather Rev. 137, 3960–3977. https://doi.org/10.1175/2009MWR2750.1

Giot, O., Termonia, P., Degrauwe, D., De Troch, R., Caluwaerts, S., Smet, G., Berckmans, J., Deckmyn, A., De Cruz, L., De Meutter, P., Duerinckx, A., Gerard, L., Hamdi, R., Van Den Bergh, J., Van Ginderachter, M., Van Schaeybroeck, B., 2016. Validation of the ALARO-0 model within the EURO-CORDEX framework. Geosci. Model Dev. 9, 1143–1152. https://doi.org/10.5194/gmd-9-1143-2016

Greene, C.A., Thirumalai, K., Kearney, K.A., Delgado, J.M., Schwanghart, W., Wolfenbarger, N.S., Thyng, K.M., Gwyther, D.E., Gardner, A.S., Blankenship, D.D., 2019. The Climate Data Toolbox for MATLAB. Geochemistry, Geophys. Geosystems 20, 3774–3781. https://doi.org/10.1029/2019GC008392

Hamdi, R., Van de Vyver, H., Termonia, P., 2012. New cloud and microphysics parameterisation for use in high-resolution dynamical downscaling: Application for summer extreme temperature over Belgium. Int. J. Climatol. 32, 2051–2065. https://doi.org/10.1002/joc.2409

IPCC, Core writing team, Pachauri, R.K., Meyer (eds.), L., 2014. Climate Change 2014: Synthesis Report. Contribution of Working Groups I, II and III to the Fifth Assessment Report of the Intergovernmental Panel on Climate Change Title. Geneva, Switzerland.

Jacob, D., 2001. A note to the simulation of the annual and inter-annual variability of the water budget over the Baltic Sea drainage basin. Meteorol. Atmos. Phys. 77, 61–73. https://doi.org/10.1007/s007030170017

Jacob, D., Elizalde, A., Haensler, A., Hagemann, S., Kumar, P., Podzun, R., Rechid, D., Remedio, A.R., Saeed, F., Sieck, K., Teichmann, C., Wilhelm, C., 2012. Assessing the transferability of the regional climate model REMO to different coordinated regional climate downscaling experiment (CORDEX) regions. Atmosphere (Basel). 3, 181–199. https://doi.org/10.3390/atmos3010181

Keetch, J.J., Byram, G.M., 1968. A Drought Index for Forest Fire Control. SE-38. Asheville, NC U.S. Dep. Agric. For. Serv. Southeast. For. Res. Pap., 35p.

Paulo, A.A., Rosa, R.D., Pereira, L.S., 2012. Climate trends and behaviour of drought indices based on precipitation and evapotranspiration in Portugal. Nat. Hazards Earth Syst. Sci. 12, 1481–1491. https://doi.org/10.5194/nhess-12-1481-2012

Pietikäinen, J.P., Markkanen, T., Sieck, K., Jacob, D., Korhonen, J., Räisänen, P., Gao, Y., Ahola, J., Korhonen, H., Laaksonen, A., Kaurola, J., 2018. The regional climate model REMO (v2015) coupled with the 1-D freshwater lake model FLake (v1): Fenno-Scandinavian climate and lakes. Geosci. Model Dev. 11, 1321–1342. https://doi.org/10.5194/gmd-11-1321-2018

Termonia, P., Fischer, C., Bazile, E., Bouyssel, F., Brožková, R., Bénard, P., Bochenek, B., Degrauwe, D., Derková, M., El Khatib, R., Hamdi, R., Mašek, J., Pottier, P., Pristov, N., Seity, Y., Smolíková, P., Španiel, O., Tudor, M., Wang, Y., Wittmann, C., Joly, A., 2018. The ALADIN System and its canonical model configurations AROME CY41T1 and ALARO CY40T1. Geosci. Model Dev. 11, 257–281. https://doi.org/10.5194/gmd-11-257-2018

Top, S., Kotova, L., De Cruz, L., Aniskevich, S., Bobylev, L., De Troch, R., Gnatiuk, N., Gobin, A., Hamdi, R., Kriegsmann, A., Remedio, A.R., Sakalli, A., Van De Vyver, H., Van Schaeybroeck, B., Zandersons, V., De Maeyer, P., Termonia, P., Caluwaerts, S., 2020. Evaluation of regional climate models ALARO-0 and REMO2015 at 0.22° resolution over the CORDEX Central Asia

domain. Geosci. Model Dev. Discuss. 1–38. https://doi.org/10.5194/gmd-2019-368

Vicente-Serrano, S.M., Beguería, S., López-Moreno, J.I., 2010. A multiscalar drought index sensitive to global warming: The standardized precipitation evapotranspiration index. J. Clim. 23, 1696–1718. https://doi.org/10.1175/2009JCLI2909.1

Xu, Z., FitzGerald, G., Guo, Y., Jalaludin, B., Tong, S., 2016. Impact of heatwave on mortality under different heatwave definitions: A systematic review and meta-analysis. Environ. Int. 89–90, 193–203. https://doi.org/10.1016/j.envint.2016.02.007

# Appendix A:

## Figures of the present characteristics and future evolution of the climatic hazards in Georgia analyzed in the frame of the CRED project

This appendix gathers the figures that integrate the information about the characteristics of the climatic hazards in the present climate and their future evolution projected by the ensemble simulations under RCP 2.6 and RCP 8.5 scenarios.

### 1. Extreme precipitation

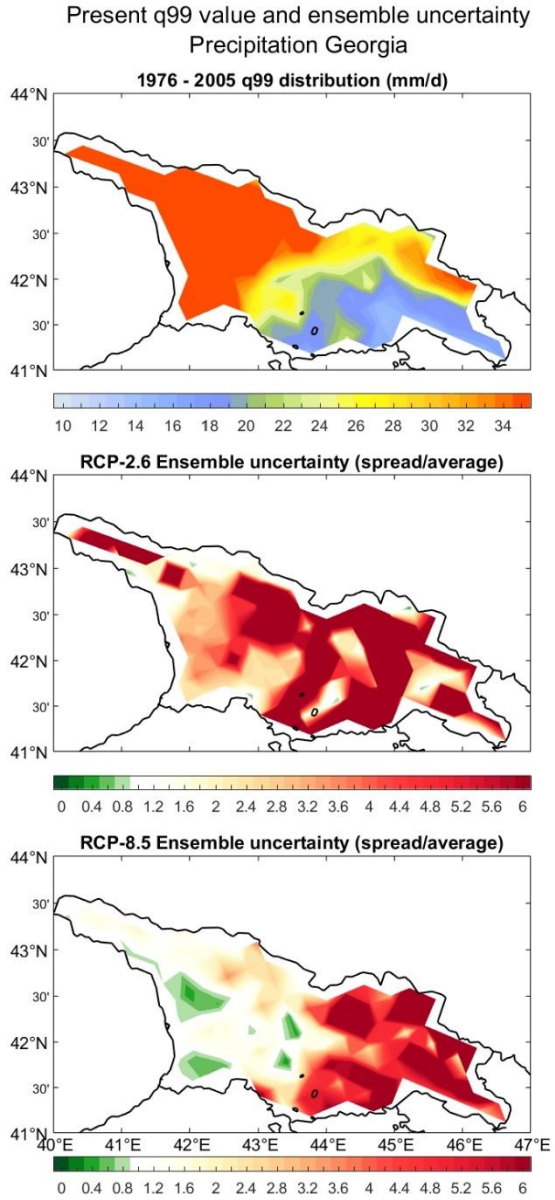


**Figure A1.** The top panel shows the average extreme precipitation values in the historical period (mm/d). The central and bottom panels show the ensemble uncertainty for the RCP 2.6 and RCP 8.5 scenarios, respectively.

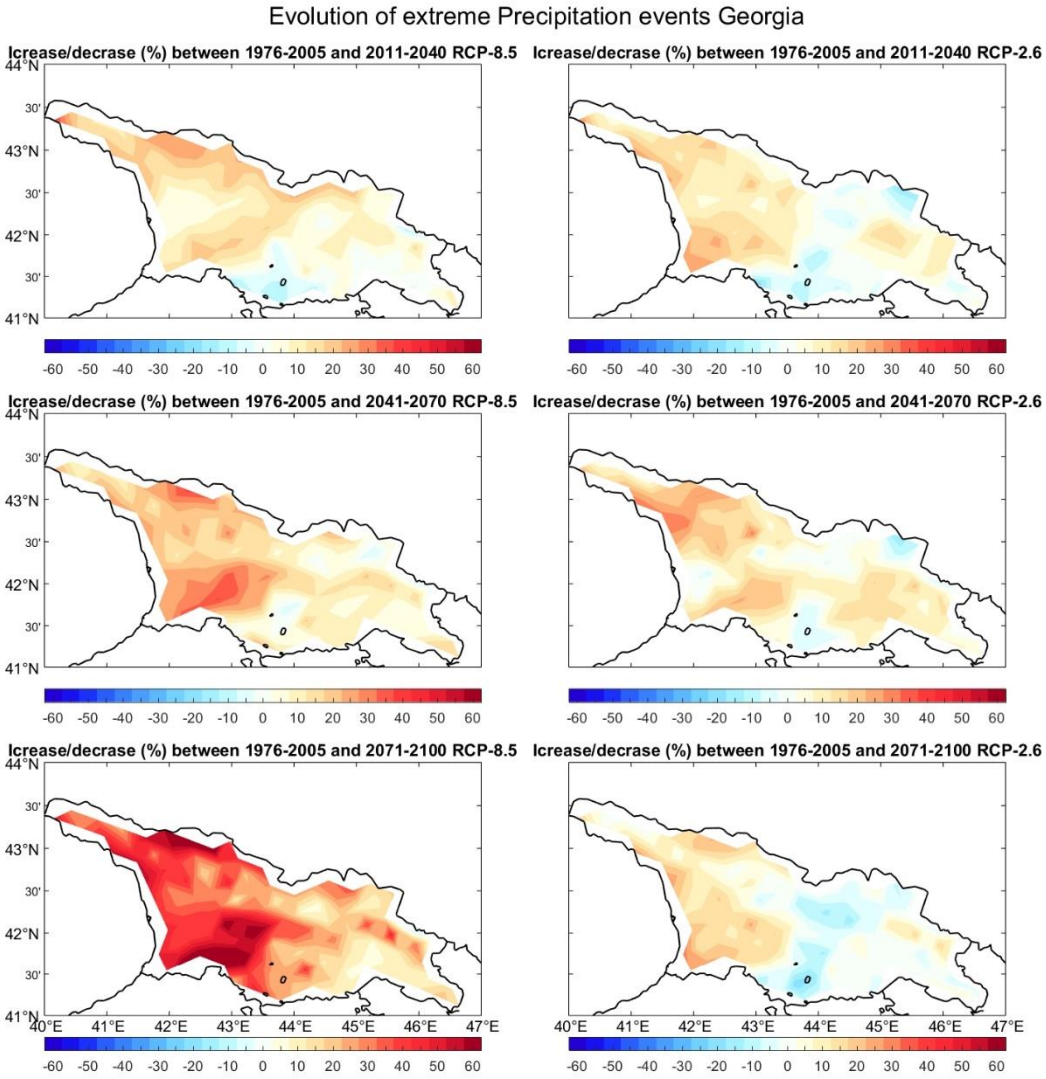


**Figure A2.** Extreme precipitation evolution in the 21st century. The left panels show the evolution under RCP 8.5 scenario and the right panels under RCP 2.6 scenario. The top panels show the average increase/decrease (in %) of the number of events per year with respect to the historical period by the beginning of the century, the center panels by midcentury and the bottom panels by the end on the century.

## 2. Extreme Temperature

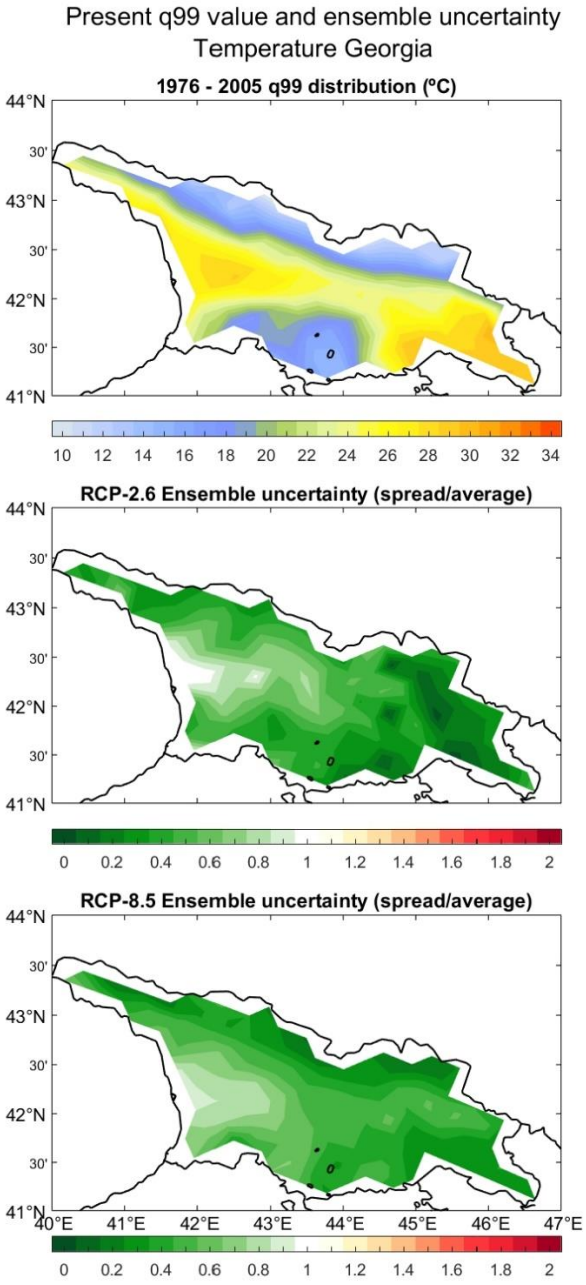


**Figure A3.** The top panel shows the average extreme temperature values in the historical period (ºC). The central and bottom panels show the ensemble uncertainty for the RCP 2.6 and RCP 8.5 scenarios, respectively.

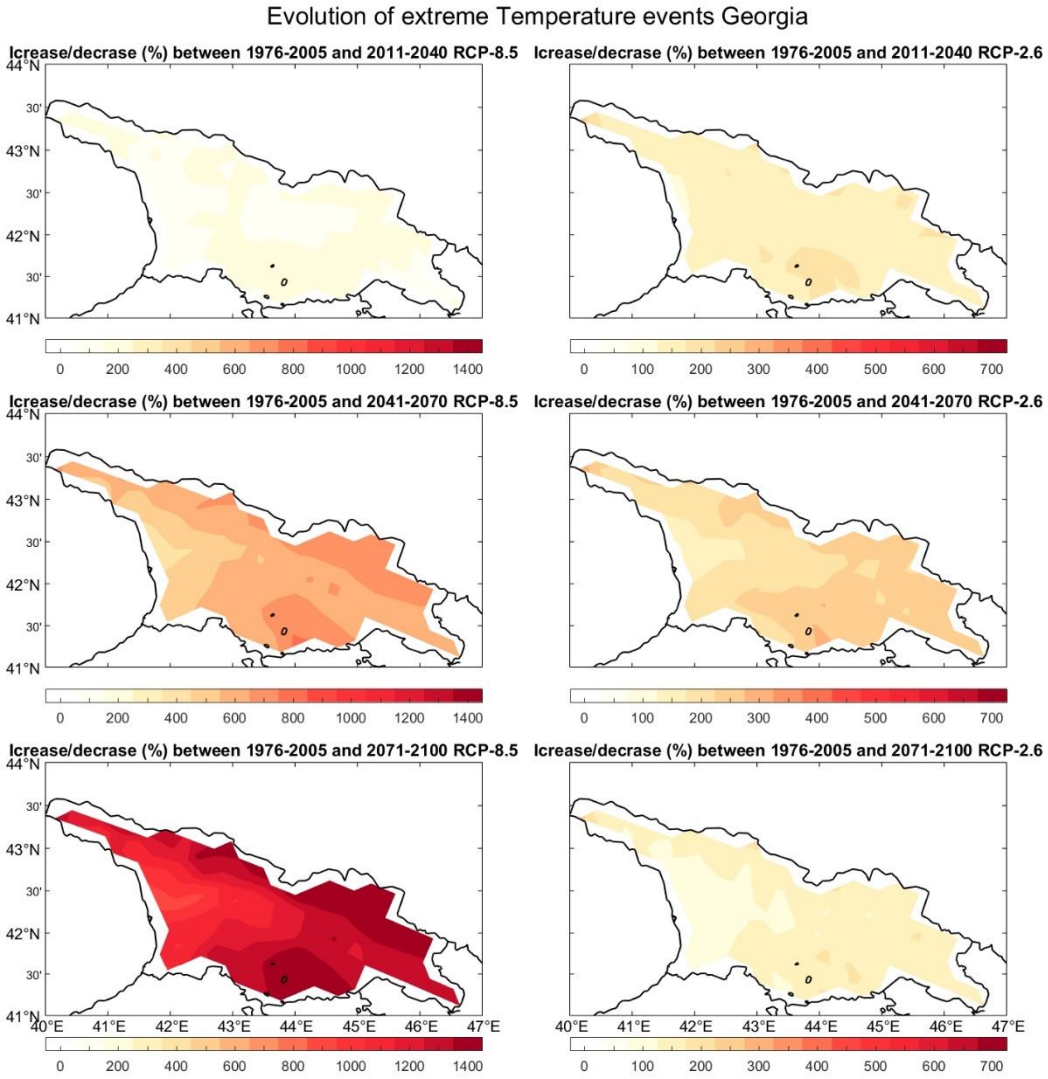


**Figure A4.** Extreme temperature evolution in the 21st century. The left panels show the evolution under RCP 8.5 scenario and the right panels under RCP 2.6 scenario. The top panels show the average increase/decrease (in %) of the number of events per year with respect to the historical period by the beginning of the century, the center panels by midcentury and the bottom panels by the end on the century.

## 3 Extreme wind events

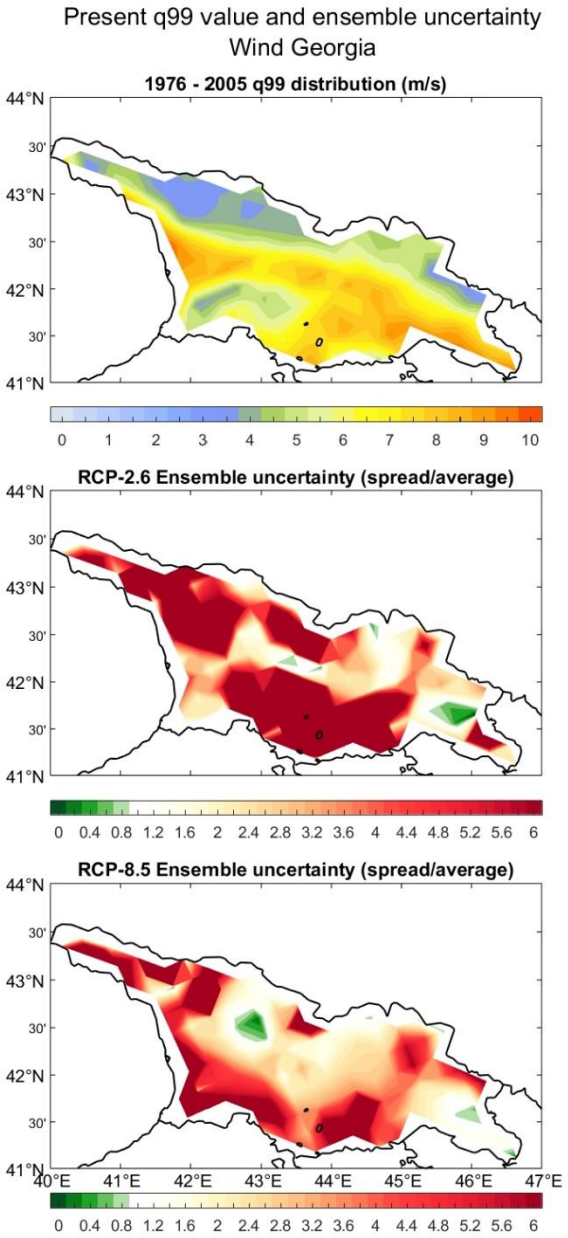


**Figure A5.** The top panel shows the average extreme wind speed values in the historical period (m/s). The central and bottom panels show the ensemble uncertainty for the RCP 2.6 and RCP 8.5 scenarios, respectively.

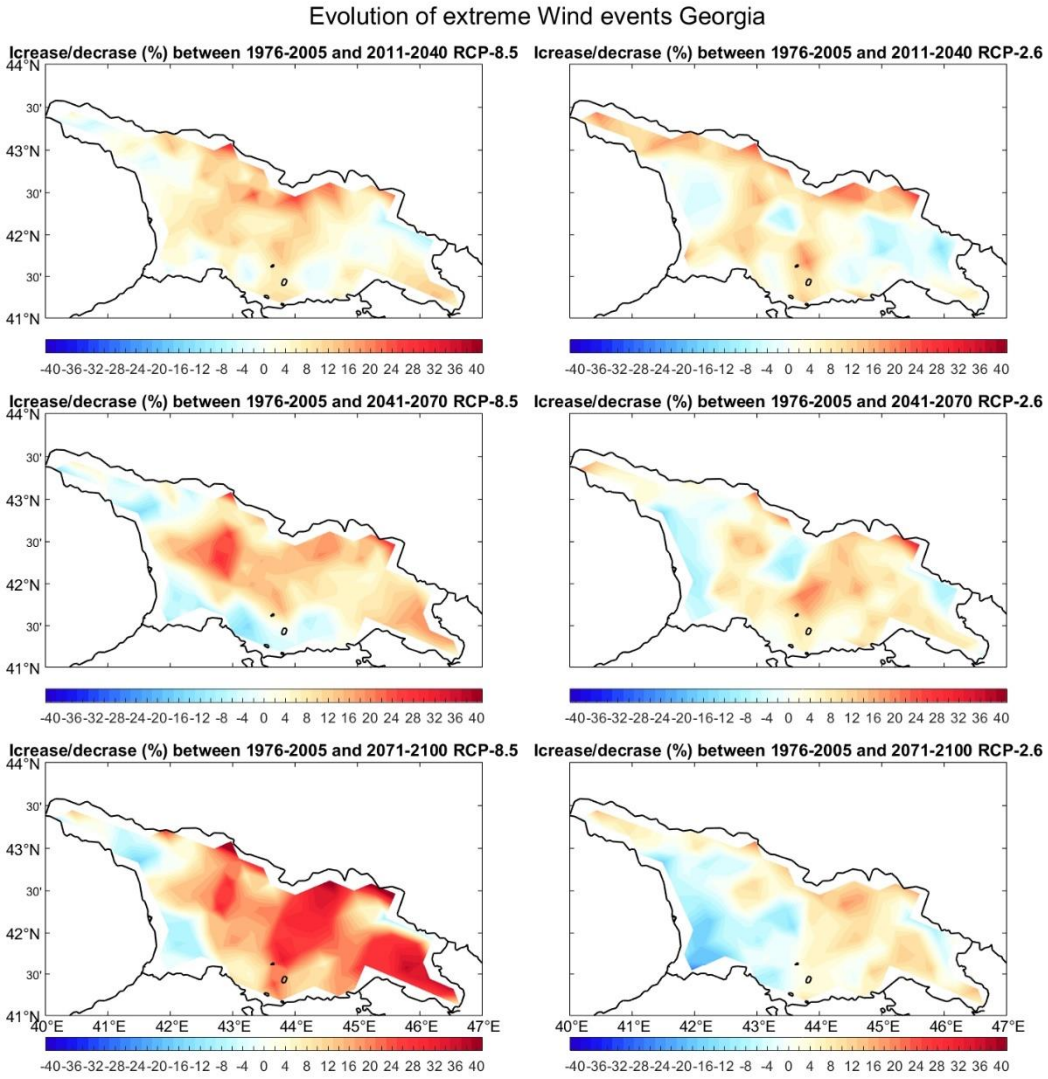


**Figure A6.** Extreme wind speed evolution in the 21st century. The left panels show the evolution under RCP 8.5 scenario and the right panels under RCP 2.6 scenario. The top panels show the average increase/decrease (in %) of the number of events per year with respect to the historical period by the beginning of the century, the center panels by midcentury and the bottom panels by the end on the century.

# 4. Heatwaves

## 4.1 Number of heatwaves

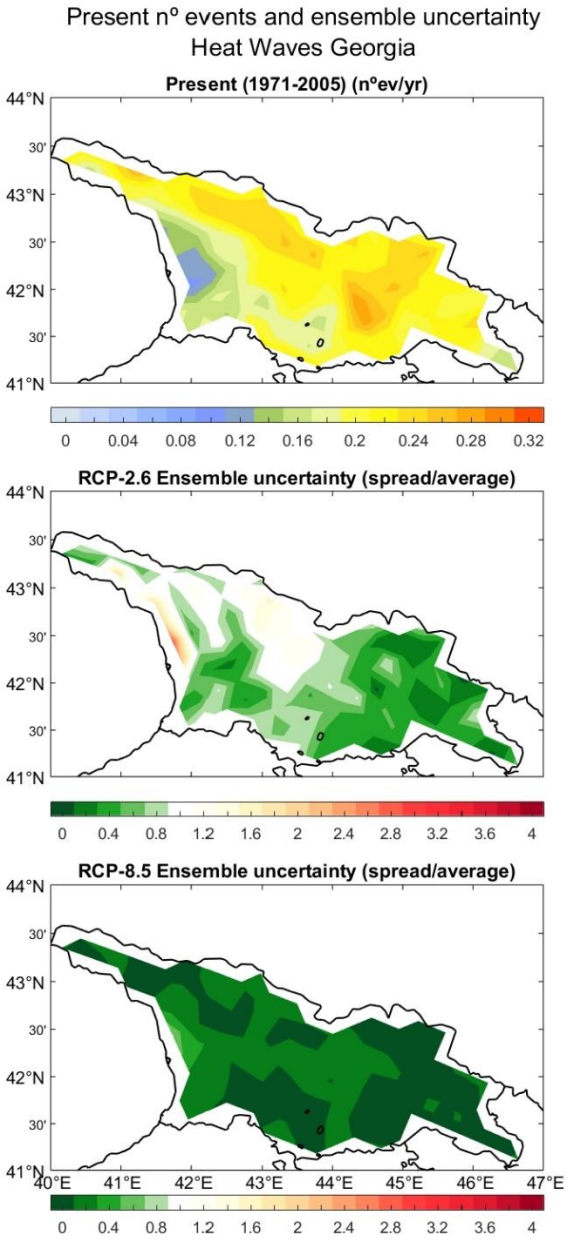


**Figure A7.** The top panel shows the average number of heatwaves per year in the historical period. The central and bottom panels show the ensemble uncertainty for the RCP 2.6 and RCP 8.5 scenarios, respectively.

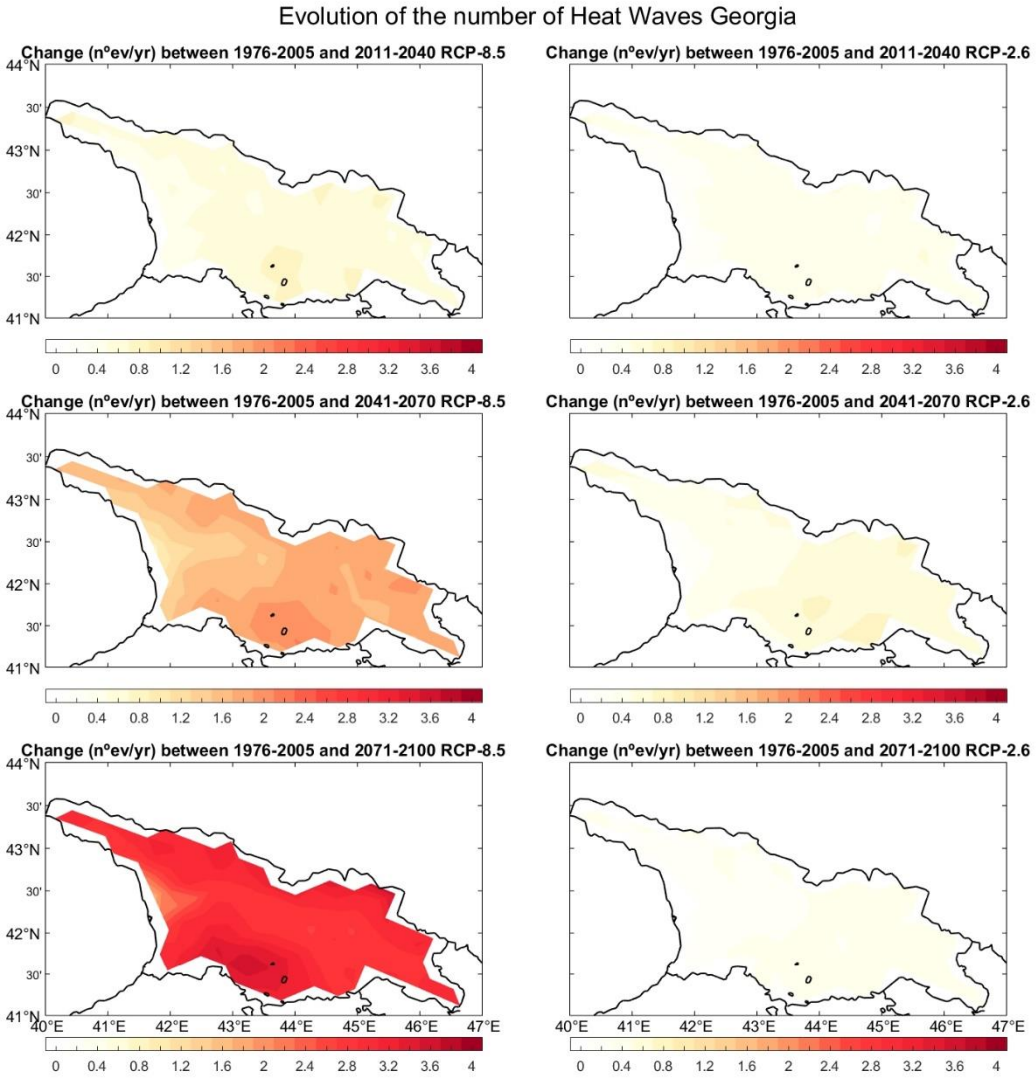


**Figure A8.** Evolution of the number of heatwaves in the 21st century. The left panels show the evolution under RCP 8.5 scenario and the right panels under RCP 2.6 scenario. The top panels show the average increase/decrease of the number of events per year with respect to the historical period by the beginning of the century, the center panels by midcentury and the bottom panels by the end on the century.

## 4.2 Intensity of the heatwaves

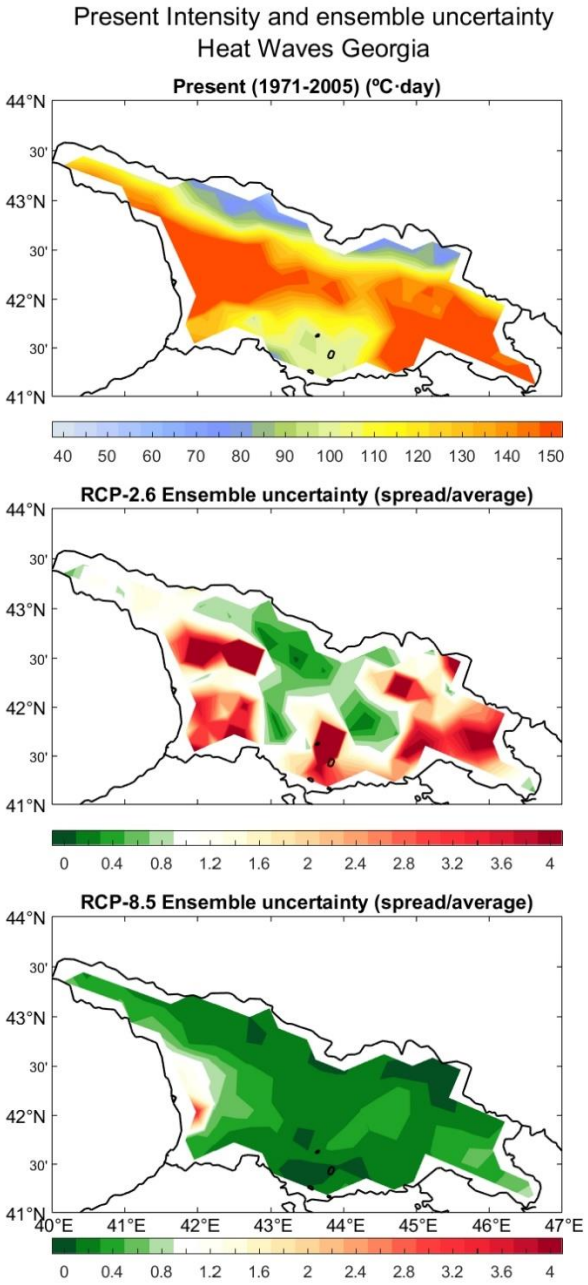


**Figure A9.** The top panel shows the average intensity of the heatwaves in the historical period (ºC·day). The central and bottom panels show the ensemble uncertainty for the RCP 2.6 and RCP 8.5 scenarios, respectively.

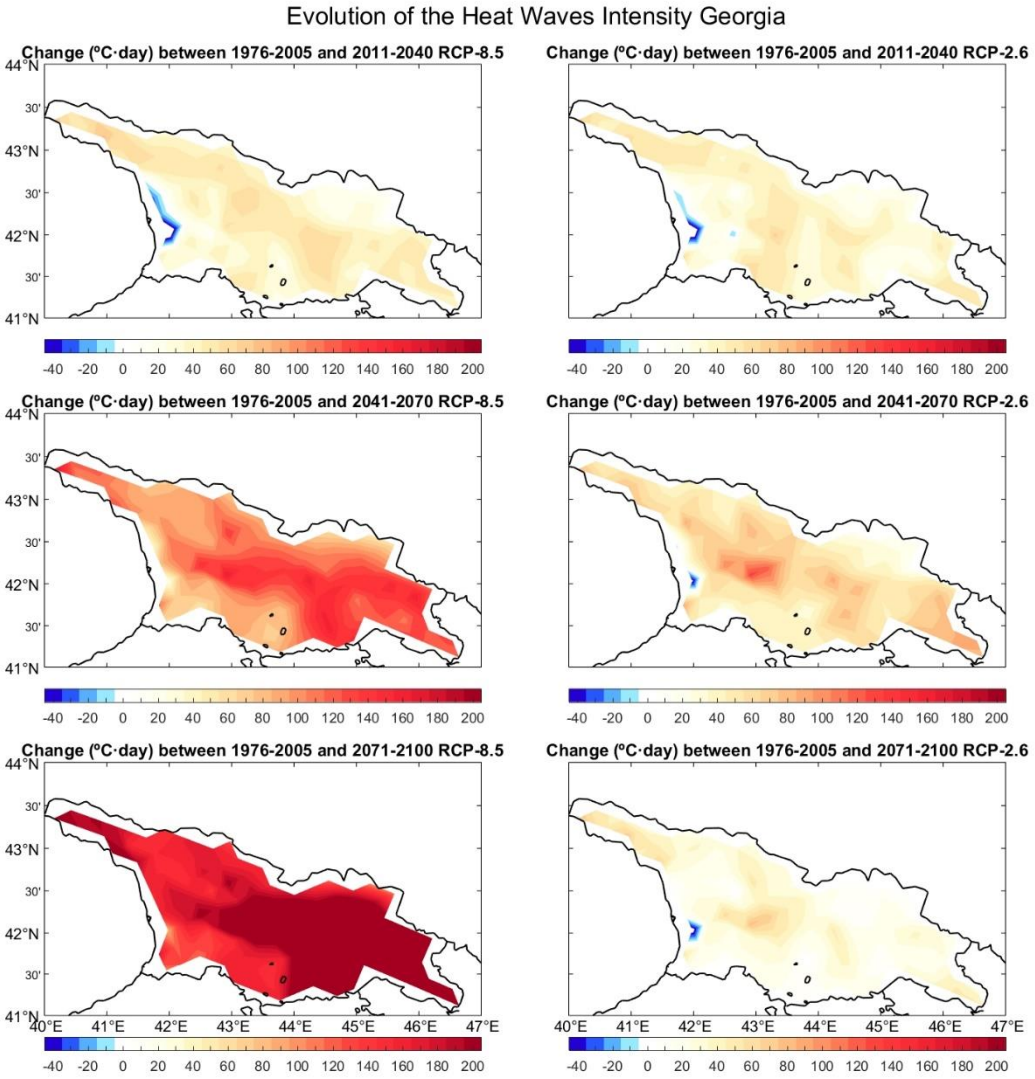


**Figure A10.** Evolution of the intensity of heatwaves in the 21st century. The left panels show the evolution under RCP 8.5 scenario and the right panels under RCP 2.6 scenario. The top panels show the average increase/decrease of the intensity (in ºC·day) with respect to the historical period by the beginning of the century, the center panels by midcentury and the bottom panels by the end on the century.

## 4.3. Duration

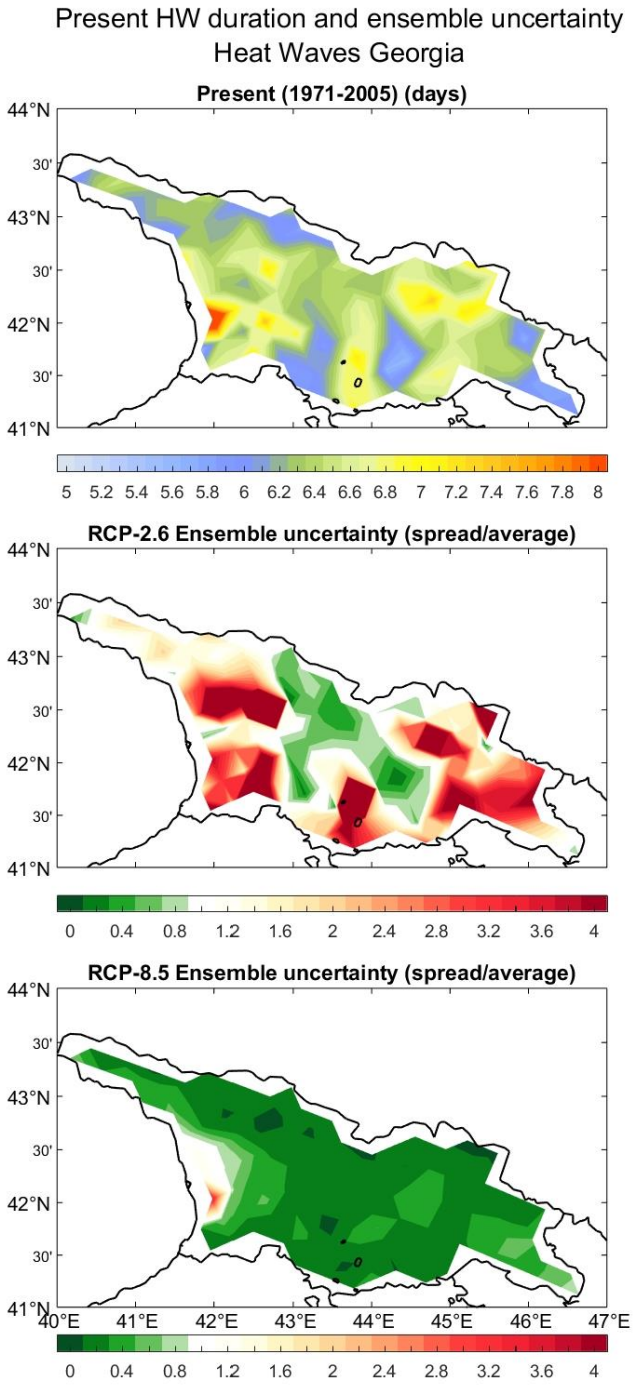


**Figure A11.** The top panel shows the average duration of the heatwaves in the historical period (days). The central and bottom panels show the ensemble uncertainty for the RCP 2.6 and RCP 8.5 scenarios, respectively.

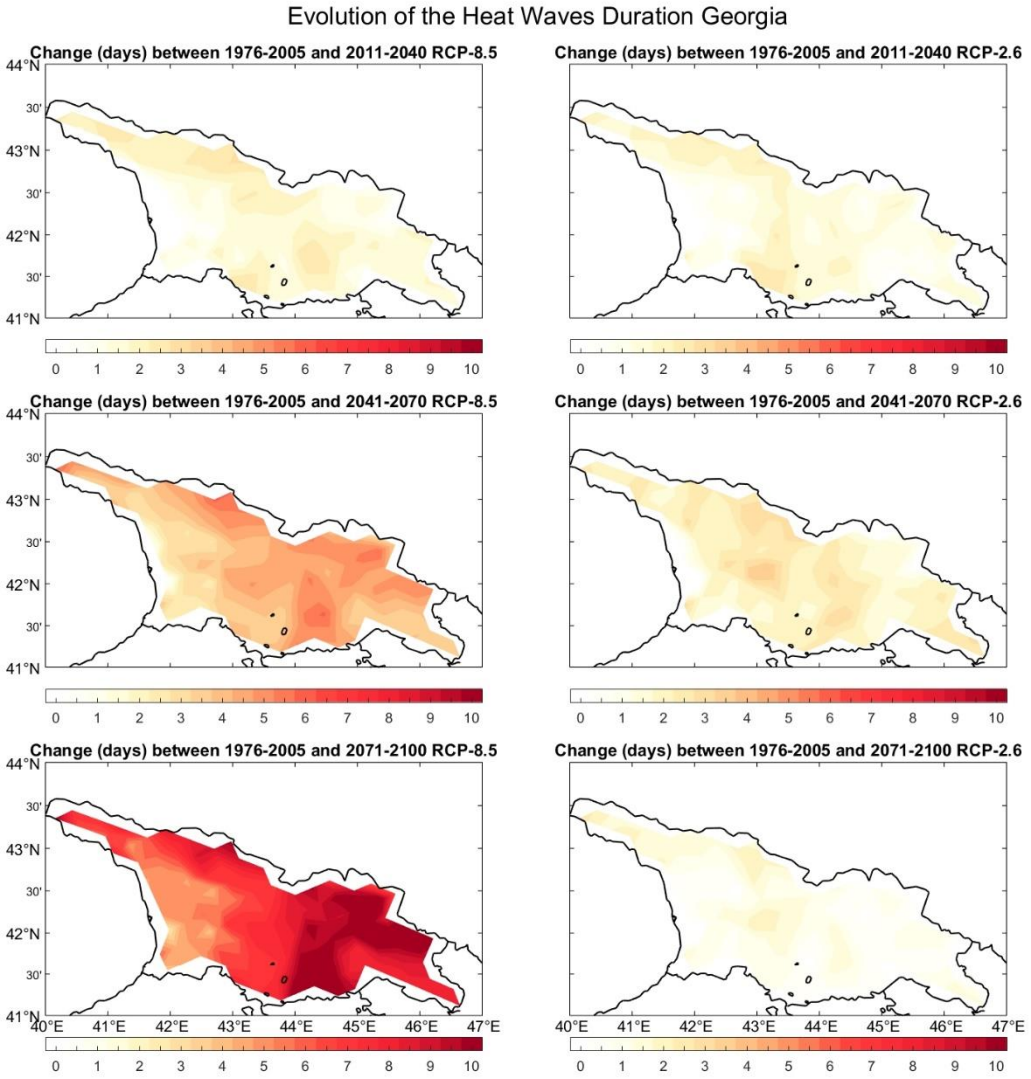


**Figure A12.** Evolution of the duration of the heatwaves in the 21st century. The left panels show the evolution under RCP 8.5 scenario and the right panels under RCP 2.6 scenario. The top panels show the average increase/decrease of the duration (days) with respect to the historical period by the beginning of the century, the center panels by midcentury and the bottom panels by the end on the century.

## 5 Droughts (SPEI)

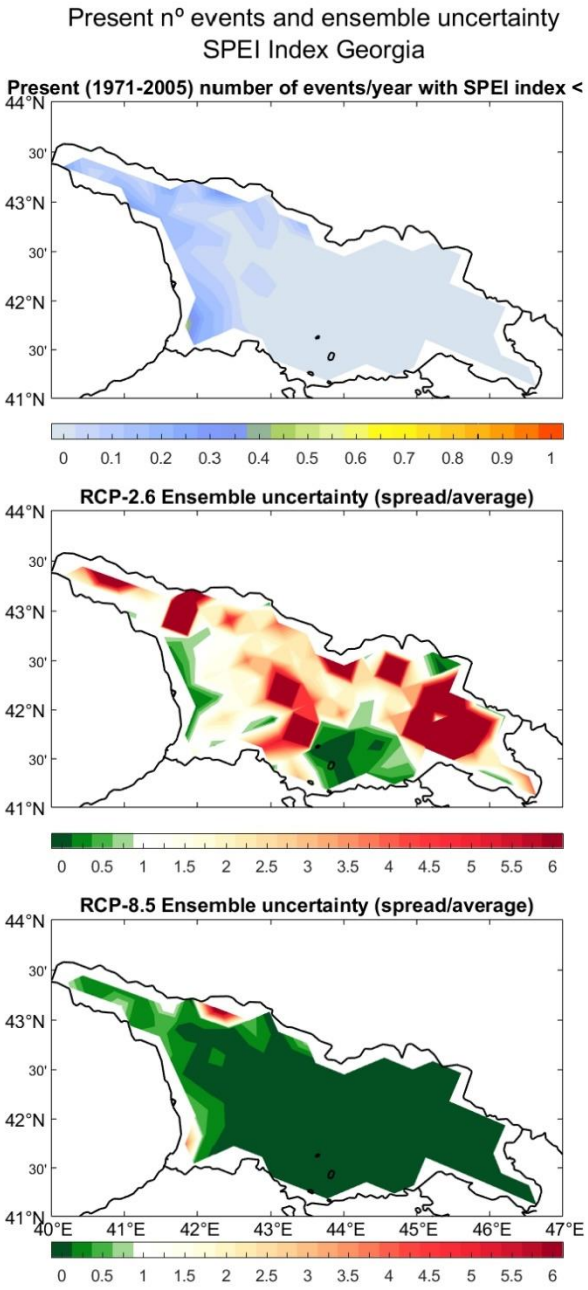


**Figure A13.** The top panel shows the average number of drought events per year (SPEI < -2) in the historical period. The central and bottom panels show the ensemble uncertainty for the RCP 2.6 and RCP 8.5 scenarios, respectively.

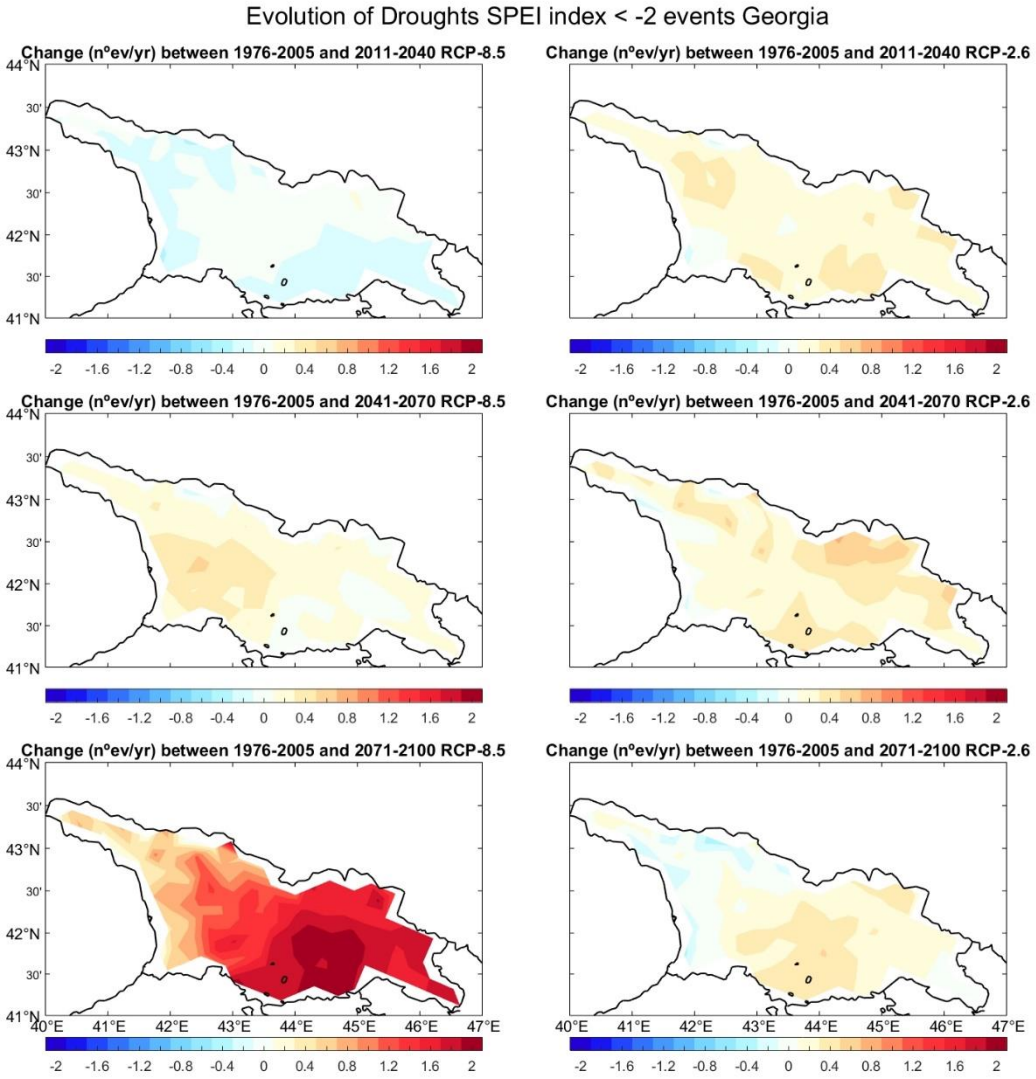


**Figure A14.** Evolution of the number of drought events per year the 21st century. The left panels show the evolution under RCP 8.5 scenario and the right panels under RCP 2.6 scenario. The top panels show the average increase/decrease number of events per year with respect to the historical period by the beginning of the century, the center panels by midcentury and the bottom panels by the end on the century.

## 6. Wildfires (KBDI)

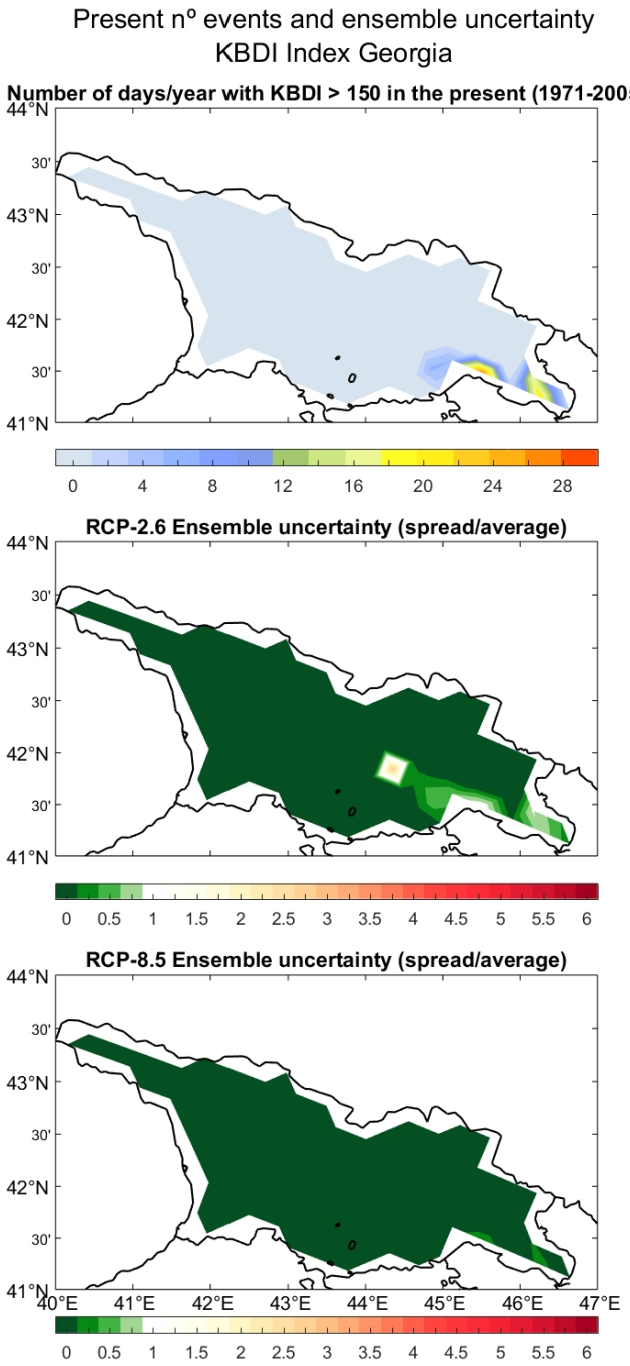


**Figure A15.** The top panel shows the average number of days per year with extreme risk of fire (KBDI > 150) in the historical period. The central and bottom panels show the ensemble uncertainty for the RCP 2.6 and RCP 8.5 scenarios, respectively.

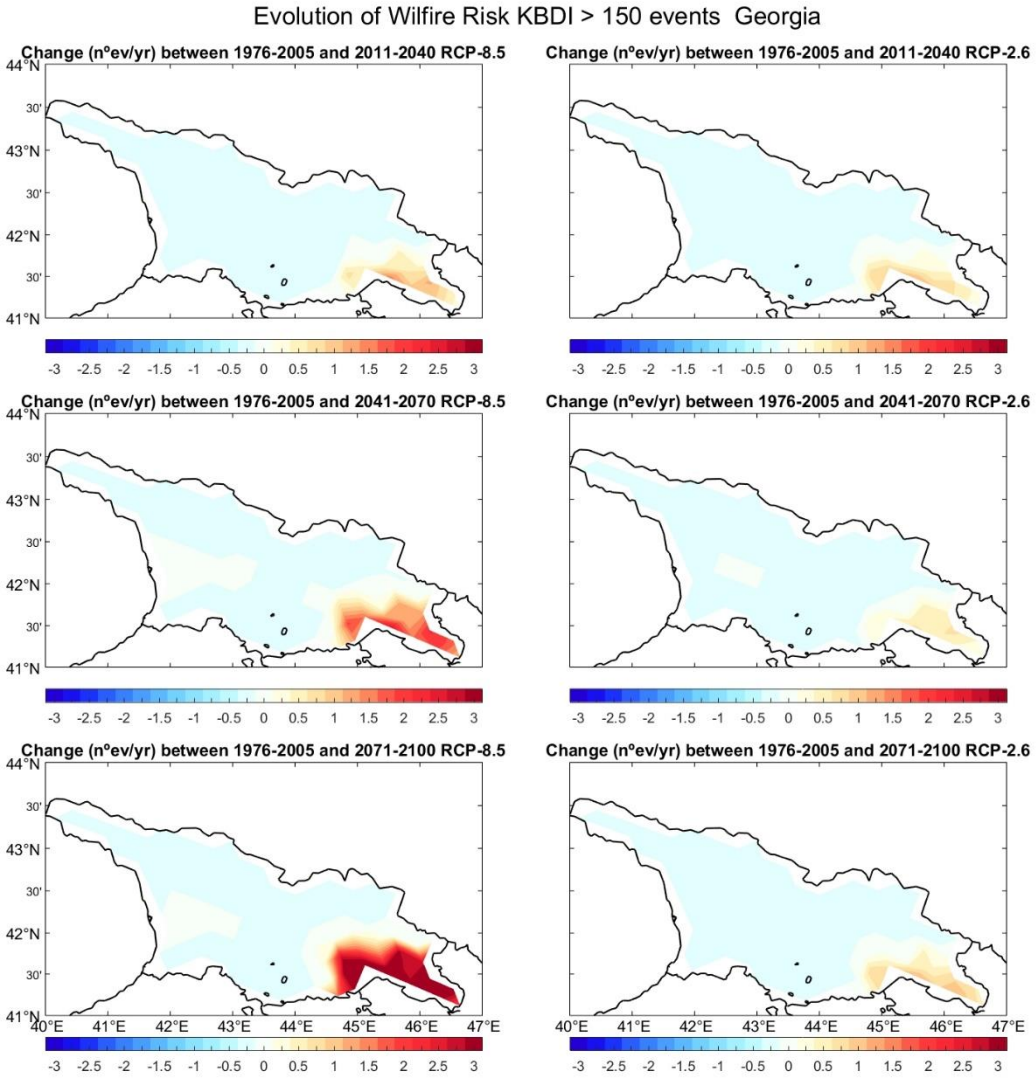


**Figure A16.** Evolution of the number of days with extreme risk of fire per year the 21st century. The left panels show the evolution under RCP 8.5 scenario and the right panels under RCP 2.6 scenario. The top panels show the average increase/decrease number of days with extreme risk of fire per year with respect to the historical period by the beginning of the century, the center panels by midcentury and the bottom panels by the end on the century.